iScience

CellPress
OPEN ACCESS

Article

# Activation of Cannabinoid Receptor 2 Prevents Colitis-Associated Colon Cancer through Myeloid Cell De-activation Upstream of IL-22 Production

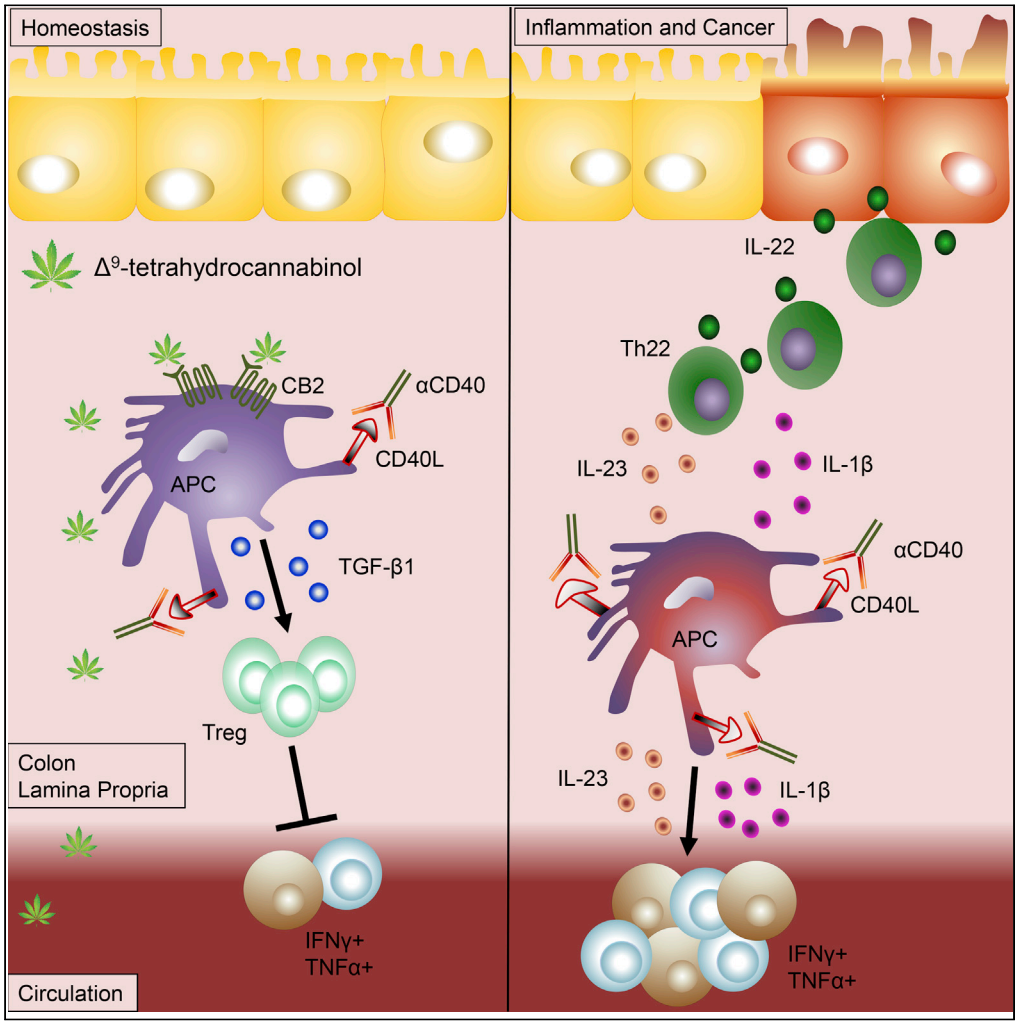


William Becker, Haider Rasheed Alrafas, Kiesha Wilson, ..., Guoshuai Cai, Mitzi Nagarkatti, Prakash S. Nagarkatti

prakash@mailbox.sc.edu

## HIGHLIGHTS

THC can prevent the development of colitis-associated colon cancer in mice

CB2 activation on immune cells dampens disease-mediated oncogenic IL-22

THC attenuates anti-CD40-induced colitis through Tregs and APCs

THC activation of CB2 on APCs reduces pro-inflammatory cytokine secretion

Becker et al., iScience 23, 101504
September 25, 2020 
https://doi.org/10.1016/j.isci.2020.101504

iScience

CellPress
OPEN ACCESS

Article

# Activation of Cannabinoid Receptor 2 Prevents Colitis-Associated Colon Cancer through Myeloid Cell De-activation Upstream of IL-22 Production

William Becker,[1] Haider Rasheed Alrafas,[1] Kiesha Wilson,[1] Kathryn Miranda,[1] Courtney Culpepper,[1] Ioulia Chatzistamou,[1] Guoshuai Cai,[2] Mitzi Nagarkatti,[1] and Prakash S. Nagarkatti[1,3,*]

## SUMMARY

**Intestinal disequilibrium leads to inflammatory bowel disease (IBD), and chronic inflammation predisposes to oncogenesis. Antigen-presenting dendritic cells (DCs) and macrophages can tip the equilibrium toward tolerance or pathology. Here we show that delta-9-tetrahydrocannabinol (THC) attenuates colitis-associated colon cancer and colitis induced by anti-CD40. Working through cannabinoid receptor 2 (CB2), THC increases CD103 expression on DCs and macrophages and upregulates TGF-β1 to increase T regulatory cells (Tregs). THC-induced Tregs are necessary to remedy systemic IFNγ and TNFα caused by anti-CD40, but CB2-mediated suppression of APCs by THC quenches pathogenic release of IL-22 and IL-17A in the colon. By examining tissues from multiple sites, we confirmed that THC affects DCs, especially in mucosal barrier sites in the colon and lungs, to reduce DC CD86. Using models of colitis and systemic inflammation we show that THC, through CB2, is a potent suppressor of aberrant immune responses by provoking coordination between APCs and Tregs.**

## INTRODUCTION

The balance between immunological tolerance and prejudice in the gut requires fine-tuned molecular signals to prevent defects that can lead to the inflammatory bowel diseases (IBDs), Crohn disease and ulcerative colitis (Lynch and Pedersen, 2016). These conditions are characterized by unrestrained gastrointestinal inflammation that begets destruction to the mucosal barrier. The burden of IBD is increasing globally, with incidence and prevalence increasing especially in Eastern and developing countries (Coward et al., 2019). It has been shown conclusively that, besides the pernicious effects of IBD, those afflicted have an increased risk of developing colorectal cancer (CRC) during their lifetime (Dyson and Rutter, 2012). Although the complete etiology of IBD is unclear, a clear genetic component underlies its development (Cho, 2008), and recent studies have fine-mapped 45 potential loci as precipitating IBD (Huang et al., 2017). Despite the progress in delineating the underlying genetic susceptibility to IBD, host genetic factors cannot account for the increasing incidence worldwide, so environmental and microbial factors and the immune response to them must be considered.

The major IBD susceptibility genes including NOD2, STAT3, and IL-23 (Cho, 2008; Huang et al., 2017; Duerr et al., 2006; de Souza and Fiocchi, 2016) are all heavily involved in immune processes. Accordingly, interleukin (IL)-23, IL-17, and IL-22 concentrations are found at higher levels in the serum and intestine of patients with IBD (Brand et al., 2006; Fujino et al., 2003). Pro-inflammatory IL-17 and IL-23 have well-defined roles in the inflammatory cascades that instigate IBD; however, the role of IL-22 is contentious. IL-22 is crucial in regulating barrier surfaces: increasing epithelial and mucosal defenses, releasing anti-microbial peptides (Parks et al., 2016), and protecting enterocyte stem cells (Gronke et al., 2019), and is necessary for the clearance of *Citrobacter rodentium* infection (Manta et al., 2013). IL-22 has also been identified as pathogenic (Eken et al., 2014), and IL-22 is a strong contender for initiating CRC by increasing epithelial cell STAT3 expression (Sun et al., 2015; Kryczek et al., 2014; Kirchberger et al., 2013). The primary producers of IL-22 in the intestines are group 3 innate lymphoid cells (ILC3s) and CD4+ Th cells that secrete IL-22 at lower levels (Dudakov et al., 2015). IL-22 production by both ILC3s and Th22 cells can be stimulated by pro-inflammatory cytokines IL-23, MCP-1, IL-1β, and IL-6 (Parks et al., 2016; Manta et al., 2013; Dudakov et al., 2015). ILC3 production of IL-22 is tightly controlled by exogenous and endogenous factors. Metabolites from food and microbes modulate transcription factors such as AhR, RORγt, and STAT3 (Kiss and Diefenbach,

[1]Department of Pathology, Microbiology and Immunology, University of South Carolina School of Medicine, Columbia, SC 29208, USA

[2]Department of Environmental Health Sciences, Arnold School of Public Health, University of South Carolina, Columbia, SC 29208, USA

[3]Lead contact

*Correspondence: prakash@mailbox.sc.edu

https://doi.org/10.1016/j.isci.2020.101504

2012). Endogenous cellular activity between ILC3s and antigen-presenting cells (APCs) can also regulate ILC3 IL-22 secretion. APCs in the intestines are the arbiters between tolerance and resistance, priming ILCs, Th cells, and gut-protective T regulatory cells (Tregs) against deemed threats. Dendritic cells (DCs) are the classical APCs and present commensal and dietary antigens to T cells in the intestines. DCs in the gut are not homogeneous. CD103+ DCs are typically tolerogenic, expressing high levels of aldehyde dehydrogenase, TGF-β1, and integrin β8 that work to induce Tregs and up-regulate CCR9 for homing to the gut (Sun et al., 2007; Merad et al., 2013; Coombes et al., 2007). However, increased CD103 expression on DCs is also thought to play a role in cross-priming virus and tumor-specific cytotoxic T cells (Hildner et al., 2008), and the role of CD103+ CD11b+ DCs is less clear, displaying a double-edged sword phenotype wherein they can behave as CD103+ DCs to secrete retinoic acid and increase Tregs, or they can induce Th17 cells (Persson et al., 2013). CD103- CD11b+ DCs act in a more classically pro-inflammatory fashion similar to macrophages. Macrophages in the gut, especially tissue-resident $CX_3CR1$+ (fractalkine receptor) macrophages (also called myeloid DCs or mononuclear phagocytes) are the dominant source of pro-inflammatory cytokines, IL-23, IL-1β, and granulocyte-macrophage colony-stimulating factor (GM-CSF) in the gut, which are potent activators of ILC3 IL-22 production, and deleting these cells decreases the proportion of IL-22-producing ILC3s (Manta et al., 2013; Longman et al., 2014).

Modulation of the endocannabinoid system (ECS) for IBD has shown promise in pre-clinical models (Whiting et al., 2015; Singh et al., 2012; Storr et al., 2009; Ke et al., 2016) and small human cohorts (Naftali et al., 2013; Lahat et al., 2012). Murine data on the ECS in CRC indicate a role for cannabinoids in preventing aberrant crypt formation through CB2 (Izzo et al., 2008), and direct apoptosis of cancer cells through CB1 or CB2 (Cianchi et al., 2008). Human data indicate that CB2 is upregulated in colorectal tumor tissue, and tumors expressing higher CB2 mRNA proliferate more (Martínez-Martínez et al., 2015). The discrepancy between observations of ECS activity in cancer can be partially accounted for by the findings that cannabinoid receptor (CB) agonists display bimodal action in cancer cell lines with proliferative responses at lower endogenous levels and apoptotic responses with higher exogenous doses (Pisanti et al., 2013). In this study we use the exogenous cannabinoid delta-9-tetrahydrocannabinol (THC) to influence the gut immune balance toward homeostasis in models of cancerous and pre-cancerous inflammation. We show THC to be an effective treatment for preventing colitis-associated colon cancer using the azoxymethane (AOM) + dextran sulfate sodium (DSS) model of colorectal tumorigenesis. We also reveal pro-tumorigenic IL-22 in the epithelial microenvironment to be reduced via THC-mediated CB2 activation on hematopoietic cells. Thus to isolate the effects of THC on the immune system and to study the interactions between gut adaptive and innate immunity to regulate IL-22 secretion, we used the anti-CD40 model, which initiates disease course independently of the microbiota or intestinal permeability to stimulate inflammation (Uhlig et al., 2006; Barthels et al., 2017). The CD40-CD154 (CD40L) interaction between APCs and T cells is important for the initiation and maintenance of adaptive immune responses (Cong et al., 2000). Blocking the CD40-CD40L interaction can be used prophylactically and therapeutically in established models of murine colitis (Polese et al., 2002). In humans, CD40+ APCs are found near CD40L+ T cells in inflamed IBD tissue (De Jong et al., 2000). Studies have identified CD40 stimulation in mice to initiate an inflammatory cascade dependent on myeloid cell production of IL-12 to provoke T cell and natural killer cell release of interferon (IFN)-γ that causes systemic inflammation, and myeloid release of IL-23 leading to colonic inflammation (Uhlig et al., 2006). In mice with intact adaptive immunity, Tregs play an important role in development and resilience to disease. LAG-3+ Tregs can reduce colitogenic CD40-stimulated CX3CR1+ macrophage secretion of IL-23 to prevent pathogenic ILC3 IL-22 production (Bauché et al., 2018). Conversely, anti-CD40 acts on CD103+ DCs to upregulate CCR7 and migrate to the mesenteric lymph node (mLN) where they undergo apoptosis, reducing RORγt+ Foxp3+ Tregs that leads to fatal T cell mediated colitis (Barthels et al., 2017). This study looks at the myriad mechanisms of innate and adaptive immunity in the gut to pinpoint how THC prevents colitis-associated colon cancer.

## RESULTS

### THC Attenuates the Progression of Colitis-Induced Colon Cancer which Is Associated with Reduction in Il-22 Production in the Epithelial Microenvironment

To induce colon cancer, we used the well-established model of carcinogen injection, AOM (10 mg/kg, intraperitoneally [i.p.]), followed by three cycles of DSS. THC (10 mg/kg, oral gavage) or vehicle (VEH, PBS:EtOH:Tween-80, in a 17:2:1 ratio) administration begun concurrently with the first cycle of DSS and was administered twice a week. THC and VEH treatment were halted after the third DSS cycle to examine the effects of THC on cancer initiation, and not the potential direct effects of THC on tumors. Disease progression and experimental schematic is detailed in (Figure 1A), revealing that mice given DSS + AOM to induce colon cancer (CC group) but treated with THC, lost less weight compared with the CC + VEH group (Figure 1A). At termination of the study, the CC + VEH group exhibited colonic tumors, whereas CC + THC showed no tumors (Figure 1B). The size of the spleen was also

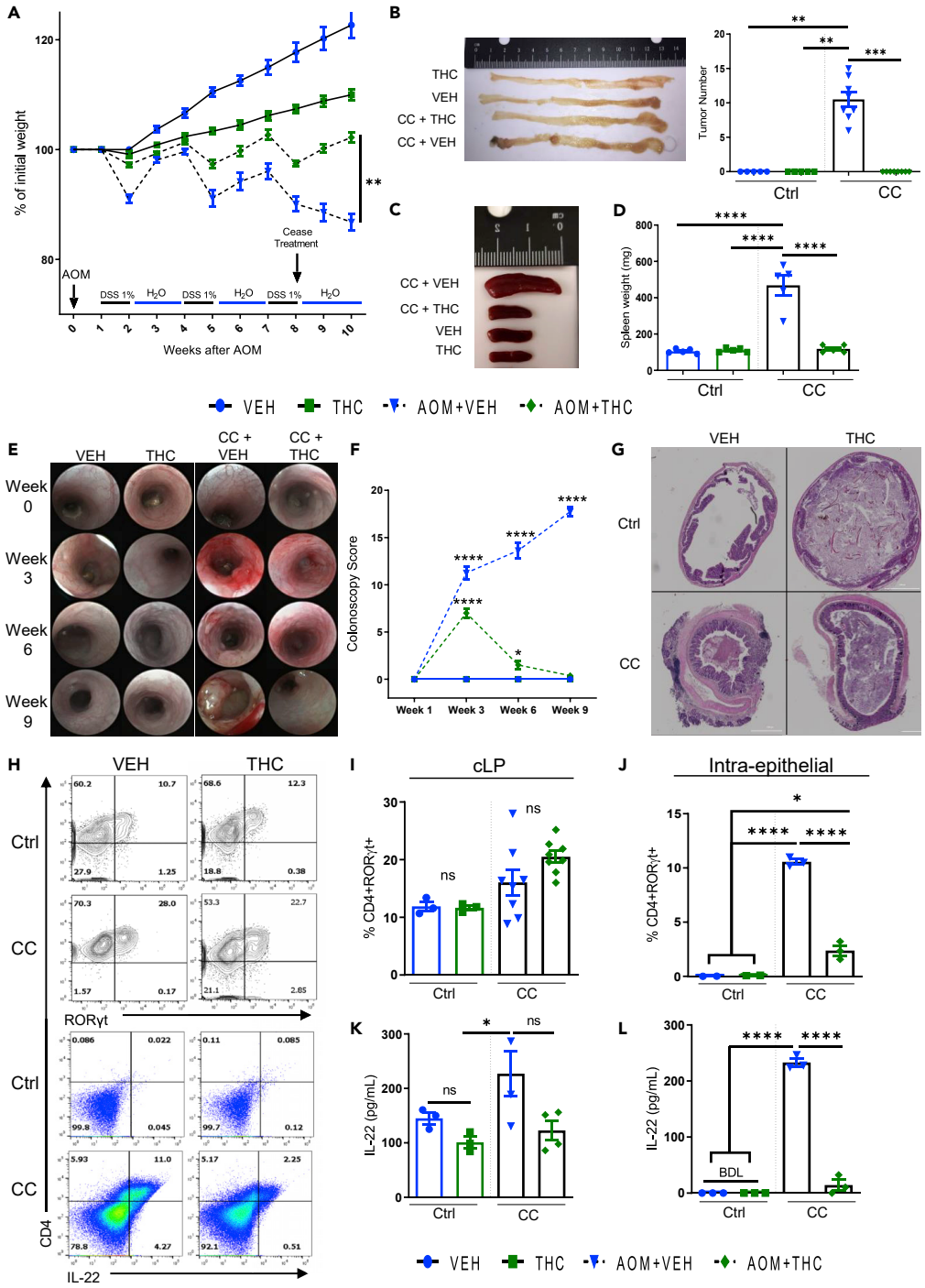


**Figure 1. Cannabinoid Receptor Activation Stems the Progression of Colitis-Induced Colon Cancer by Reducing IL-22 Production in the Epithelial Microenvironment**

To induce colitis-associated colon cancer (CC), mice were given a single injection of AOM, i.p. (10 mg/kg), then 1 week later treatment started concurrently with the induction of the first cycle of colitis with 2% DSS in the drinking water. Weeklong cycles of DSS (2%) were followed by 2 weeks of regular drinking water for 3 cycles lasting 9 weeks. Treatment with VEH (10% EtOH in PBS-Tween-80), THC (10 mg/kg), or a combination of THC and CBD (10 mg/kg, both) was given twice a week until the last DSS cycle was completed, and then treatments were halted to monitor the effects of cannabinoids on induction of cancer, not the direct effects of the cannabinoids on cancer itself. Control mice were treated twice weekly, but disease was not induced (ctrl).

**Figure 1. *Continued***

(A) Diagram showing percent weight change, treatment schedule, and disease course. (n = 5, ctrl groups; n = 7–9 CC groups).

(B) Representative photograph and number of tumors in each colon at sacrifice. Data are from one experiment representative of two independent experiments and presented as mean ± SEM; **p < 0.01, ***p < 0.001 by Kruskal-Wallis test with a Dunn's multiple comparisons test.

(C and D) (C) Representative photograph and (D) quantification of spleen weights from indicated mice at sacrifice.

(E and F) Colonoscopies were performed throughout the experiment, and representative images are shown in (E) and quantified in (F) (n = 5–8, ctrl groups; n = 8 CC groups).

(G) Representative H&E images of colons at sacrifice. cLP and intra-epithelial cell fraction (IEC) was isolated at sacrifice and stained for CD4+ RORγt+ and CD4+ IL-22+ cells.

(H) Representative contour plots displaying CD4+ RORγt+ Th17 cells (gate: Live, CD45+ CD3+ CD4+) in the cLP (top two panels) and CD4+ IL-22+ Th22 cells (gate: Live, CD45+ CD3+) in the IEC fraction (bottom two panels).

(I and J) Quantification of percentages from flow cytometry plots in (H), deriving from the (I) clP and (J) IEC (n = 3, ctrl groups; n = 3–8, CC groups).

(K and L) 1 × $10^6$ cells deriving from the (K) cLP or (L) IEC layers from indicated groups were plated overnight, supernatants were collected, and subjected to ELISAs for IL-22 (n = 3–4).

Each symbol represents an individual mouse. Data are from one experiment representative of two independent experiments and presented as mean ± SEM NS, not significant: *p < 0.05, **p < 0.01, ***p < 0.001, ****p < 0.0001 by two-way ANOVA with Tukey's multiple comparisons test.

increased in CC + VEH group, whereas THC treatment led to a significant decrease in spleen size (Figures 1C and 1D). Colonoscopies and H&E staining of colons revealed reduction in inflammatory severity and tumor induction in CC + THC group when compared with CC + VEH (Figures 1E–1G). Because chronic upregulation of IL-22 leads to cancer development, and CC + THC mice developed no tumors, we looked at immune parameters specifically, IL-22. IL-22 is a cytokine produced mainly by Th22 cells and ILCs in the gut critical to the development, maintenance, and stemness of inflammation-induced colon cancer (Sun et al., 2015; Kryczek et al., 2014; Kirchberger et al., 2013). To characterize the immune cell populations, the colonic lamina propria (cLP) cells and intra-epithelial cells (IECs) were subjected to flow cytometric analysis. Gating strategies are detailed in Figures S1A–S1D. The CC + VEH group had a significant increase in CD4+IL-22+ Th22 cells in the IEC of the colon compared with CC + THC, whereas there was no change in cLP CD4+ RORγt+ cells (Figures 1H–1J). Taking the cells from the cLP and IEC and plating them overnight to collect supernatants revealed that the increase in IL-22 seen in the CC + VEH group in the colonic microenvironment was coming specifically from cells in the IEC (Figures 1K and 1L), not the cLP. The aforementioned data demonstrated that THC prevents the development of colon cancer in DSS + AOM model and that this is associated with decrease in IL-22-producing IECs.

## Hematopoietic and Non-hematopoietic Cells Contribute to THC-Mediated Colitis Protection, but Hematopoietic Cells Are Necessary for Reducing IL-22 Production

To resolve whether CB expression on immune cells or non-hematopoietic cells were responsible for the favorable effects of THC and to determine the mechanism through which THC can reduce tumorigenic IEC IL-22 secretion, wild-type (WT) mice were myeloablated and reconstituted with bone marrow (BM) of CB2KO mice (CB2KO→WT) or WT BM (WT→WT), because the vast majority of CB expression on immune cells is CB2. Then we induced acute colitis with an injection of AOM and a single cycle of DSS to model the early stages of tumorigenesis before macroscopic tumor development but where hallmark body weight loss, colon shortening, and inflammation are present. In both groups that received THC, DSS-induced weight loss and colon shortening was abrogated compared with VEH controls, and colon shortening was more pronounced in the CB2KO → WT group (Figures 2A and 2B). Interestingly, CB2KO→WT mice given THC had reduced Th22 cells in the cLP compared with VEH and WT→WT mice, but only WT→WT mice given THC had reduced IEC Th22 cells (Figures 2C and 2D). cLP ILC3 secretion of IL-22 was unchanged at the end of the experiment (Figure S1E). The effect of THC was not a direct effect on Th22 cells because Th22 polarization of naive cells in the presence of THC did not affect secretion of IL-22 (Figure 2E). Because we showed that THC can abrogate the induction of aberrant IL-22 in acute and chronic models of tumorigenesis and that the effect is independent of direct effects of THC on Th22 generation, we shifted to a model where the stimulation of IL-22 production is mediated by myeloid cell production of pro-inflammatory cytokines.

## THC Treatment Reduces Colonic and Systemic Inflammatory Severity Induced by αCD40

To interrogate the mechanism through which THC reduces IL-22 production in the intestines, we moved to the anti-CD40 (αCD40) model of colitis. αCD40 injection causes acute colitis dependent on IL-22 production (Eken et al., 2014) and systemic inflammation that presents with acute wasting disease and inflammatory cell

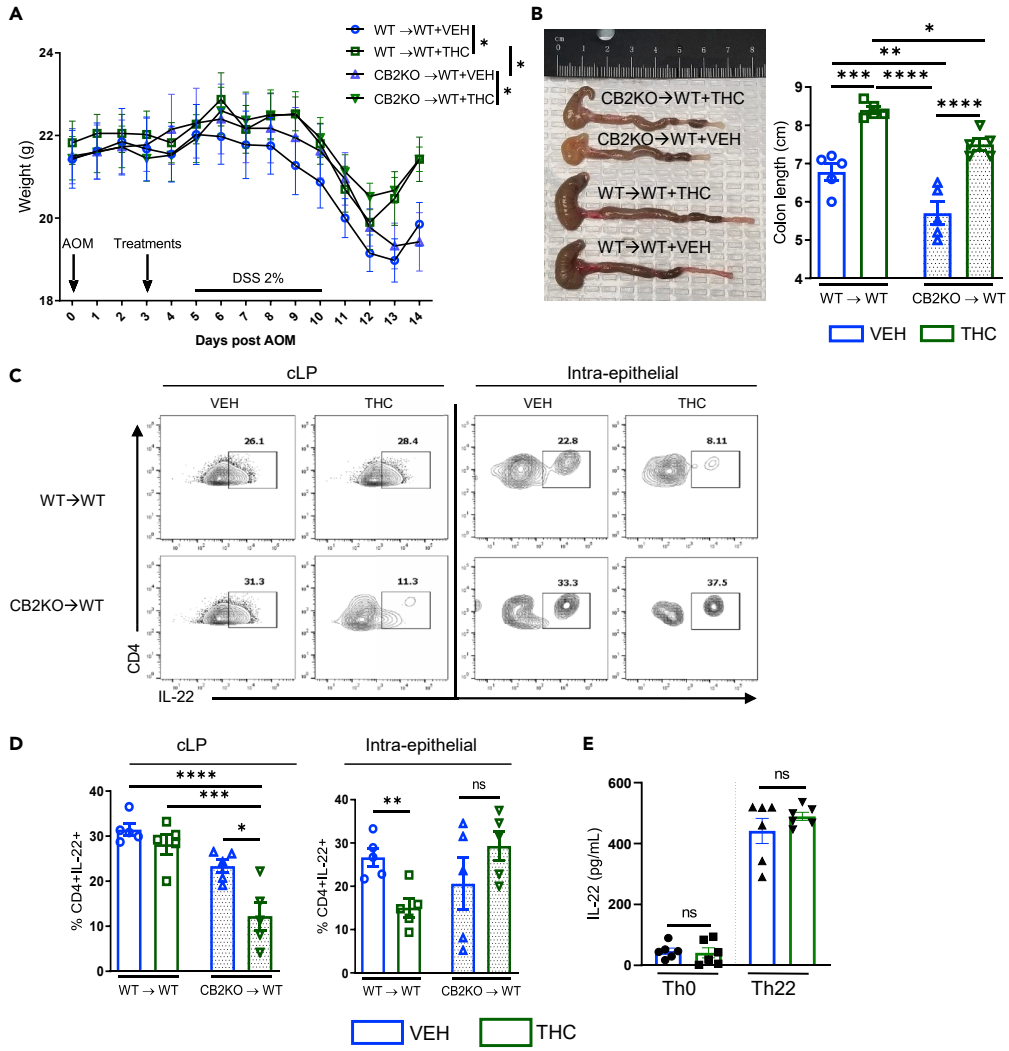


**Figure 2. Hematopoietic and Non-hematopoietic Cells Contribute to THC-Mediated Colitis Protection, but Hematopoietic Cells Are Necessary for Reducing IL-22 Production**

WT mice were myeloablated via two doses of 600 cGy separated by 3 h, then immune reconstitution was accomplished by transfer of bone marrow cells from WT (WT → WT) or Cnr2−/−, CB2 knockout (CB2 → WT) mice.

(A) Body weight throughout disease course (n = 4–5).

(B) Colon lengths at termination of the experiment.

(C and D) (C) Representative contour plots displaying CD4+ IL-22+ Th22 cells (gate: Live, CD45+ CD3+) in the cLP IEC fraction. (D) Quantification of CD4+ IL-22-expressing cells in the colonic lamina propria and epithelial fractions (n = 4–5).

(E) Naive CD4+ T cells were isolated from individual mice and plated under Th0- or Th22-polarizing conditions with VEH or THC (10μM) for 3 days. Supernatants were collected and subjected to ELISA for IL-22 (n = 6).

Each symbol represents an individual mouse. Data are from one experiment representative of two independent experiments and presented as mean ± SEM; NS, not significant; *p < 0.05, **p < 0.01, ***p < 0.001, ****p < 0.0001 by two-way ANOVA with Tukey's multiple comparisons test.

hyperactivation. THC (10 mg/kg, oral gavage) administration beginning 3 days before disease induction could not reduce the body weight loss associated with disease onset (Figure S1F). THC reduced splenomegaly occurring 7 days post- αCD40 injection (Figure 3A) and reduced circulating pro-inflammatory cytokines IFNγ, IL-17A, IL-22, and TNFα at peak of disease on day 3; Th2-related cytokines were unchanged (Figures 3B and 3C). Histologically, THC reduced the inflammatory cell infiltrate and damage caused by αCD40 in the colon and liver (Figure 3D). This effect was seen grossly in the colons via colonoscopy (Figures 3E and 3F); αCD40-mediated liver damage was measured by looking at aspartate aminotransferase (AST) and alanine aminotransferase (ALT) enzymatic activity in the serum. αCD40 mice given VEH controls had higher AST activity at day 3 than IgG controls,

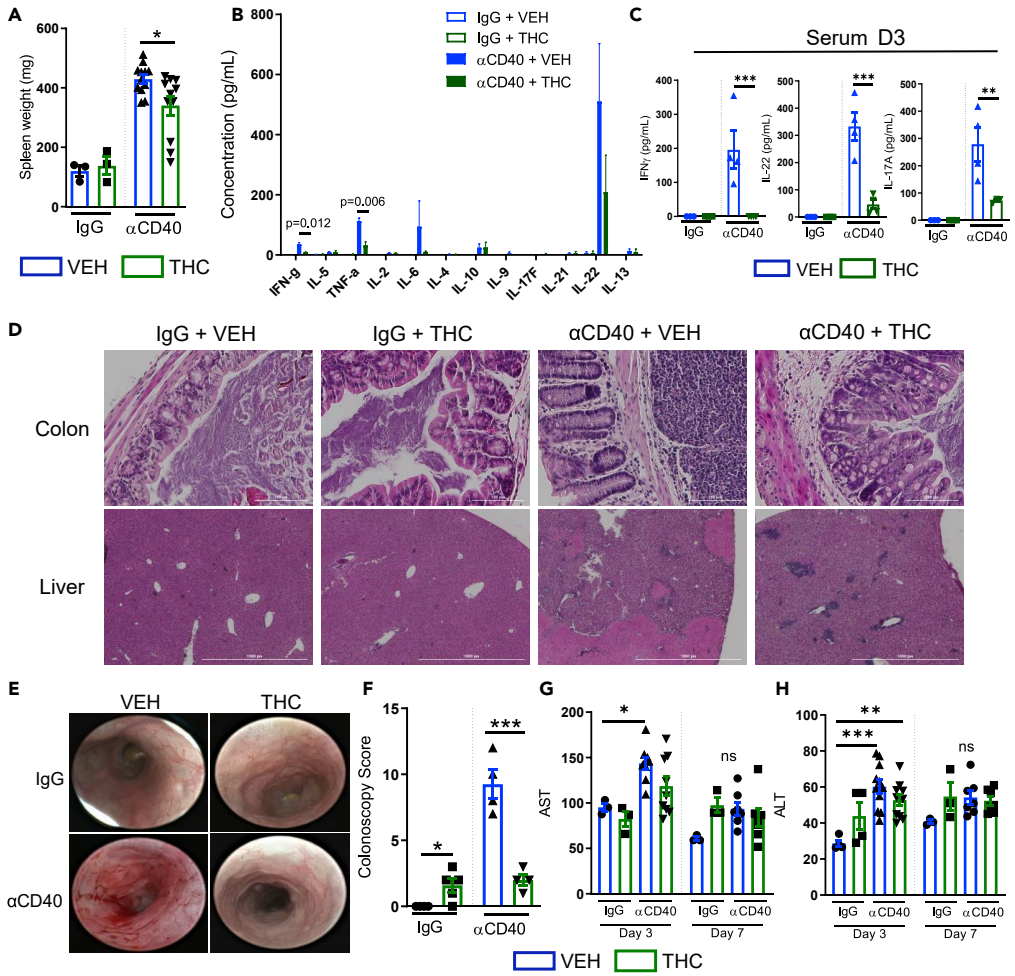


**Figure 3. THC Treatment Reduces Colonic and Systemic Inflammatory Severity Induced by αCD40**

Mice were pre-treated daily with VEH or THC (10 mg/kg) for 3 days before intraperitoneal injection of rat anti-mouse IgG (control) or rat anti-mouse αCD40 (200 μg, clone FGK4.5 in PBS) and treatment was continued for 7 days post-disease induction to monitor progression of inflammatory severity.

(A) Spleen weight (n = 3–10).

(B) On day 3, blood was collected via retro-orbital bleed and serum was separated and subjected to Legendplex assay for serum T helper cytokine levels (n = 3 per group).

(C) ELISAs for IFNγ, IL-22, and IL-17A from serum collected at day 3 from mice that received treatment or VEH 3 days before disease induction.

(D) Representative H&E images of colons (upper row, 20X) and livers (bottom row, 4X).

(E and F) (E) Representative images from colonoscopies performed on day 3 and their quantification (F) (n = 4 per group).

(G and H) Quantification of (G) AST and (H) ALT activity levels measured from serum at day 3 and day 7 post αCD40 injection.

Each symbol represents an individual mouse. Data are from one experiment representative of four independent experiments and presented as mean ± SEM. NS, not significant; *p < 0.05, **p < 0.01, ***p < 0.005 by two-way ANOVA with Tukey's multiple comparisons test.

and αCD40 mice given THC did not exhibit this increase; however, both VEH- and THC-treated mice had higher ALT activity than IgG controls at day 3 (Figures 3G and 3H).

## THC Treatment Reduces Colonic Inflammatory Cell Infiltrate and Increases Lamina Propria Tregs

We next sought to investigate the cellular mechanisms in the colon that THC acts through to reduce colonic inflammation induced by αCD40. THC treatment in αCD40 mice resulted in reduced mesenteric

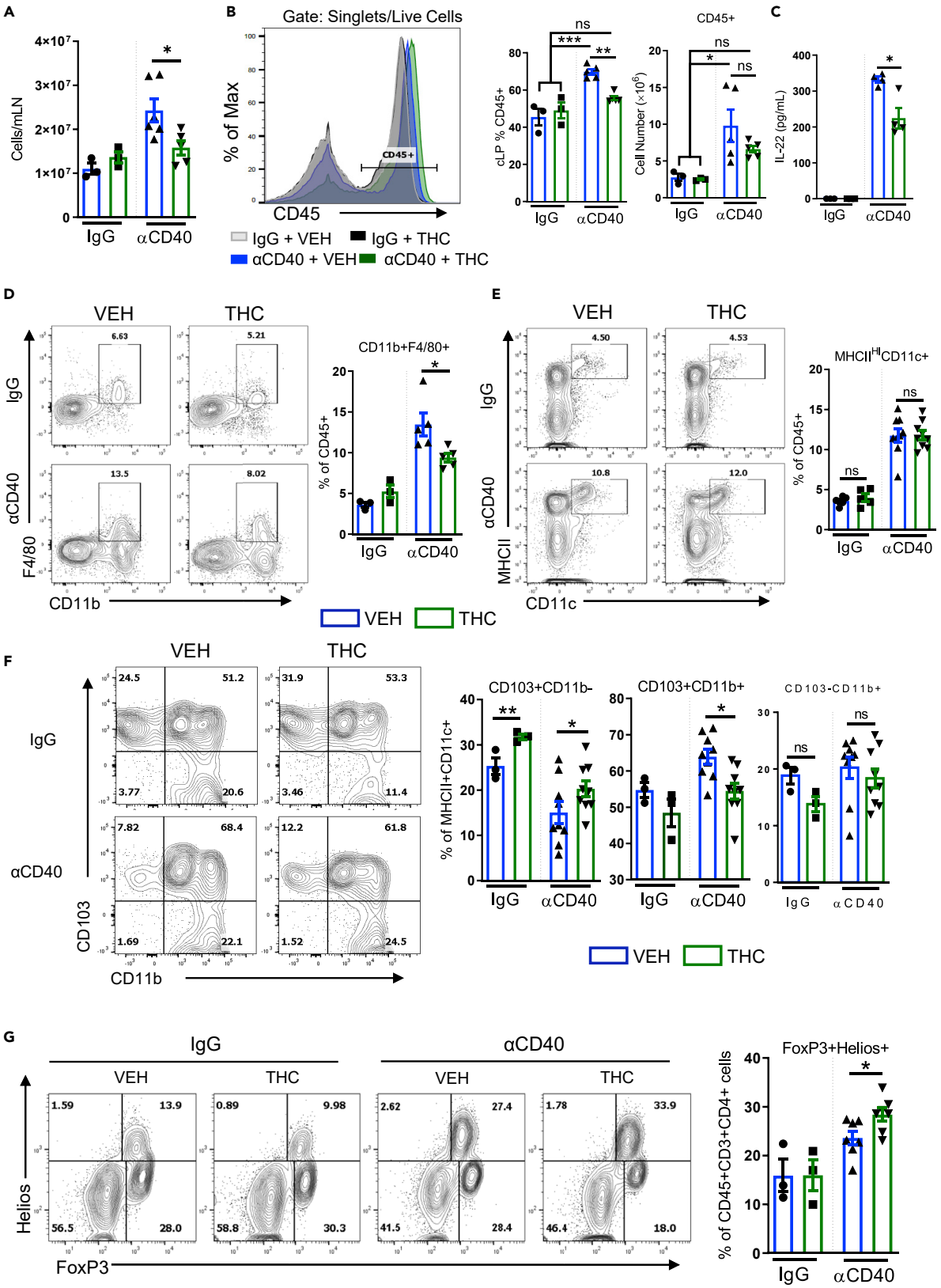
A
Cells/mLN
IgG
αCD40
B
Gate: Singlets/Live Cells
% of Max
CD45+
CD45
IgG + VEH
IgG + THC
αCD40 + VEH
αCD40 + THC
cLP % CD45+
CD45+
Cell Number (×10^6)
C
IL-22 (pg/mL)
D
VEH
THC
IgG
αCD40
F4/80
CD11b
6.63
5.21
13.5
8.02
CD11b+F4/80+
% of CD45+
VEH
THC
E
4.50
4.53
10.8
12.0
MHCII
CD11c
MHCII^HiCD11c+
F
24.5
51.2
3.77
20.6
31.9
53.3
3.46
11.4
7.82
68.4
1.69
22.1
12.2
61.8
1.52
24.5
CD103
CD103+CD11b-
CD103+CD11b+
CD103-CD11b+
% of MHCII+CD11c+
G
Helios
FoxP3
1.59
13.9
56.5
28.0
0.89
9.98
58.8
30.3
2.62
27.4
41.5
28.4
1.78
33.9
46.4
18.0
FoxP3+Helios+
% of CD45+CD3+CD4+ cells

**Figure 4. THC Treatment Reduces Colonic Inflammatory Cell Infiltrate and Increases Lamina Propria Tregs**

(A) Absolute mesenteric lymph node cell number (n = 3–6).

(B) Representative flow cytometry overlaid histograms, percentages, and absolute cell number of CD45+ cells from the colonic lamina propria of indicated mice.

(C) ELISA results for IL-22 from cLP supernatants recovered from indicated mice on day 7 (n = 3–4).

(D–F) (D) Representative flow cytometry contour plots of macrophages (gate: Live, CD45+) (n = 3–5), (E) dendritic cells (gate: Live, CD45+) (n = 5–8), and (F) cLP dendritic cell subsets on day 7 (gate: Live, CD45+ MHCII$^{HI}$CD11c+) (n = 3–9).

(G) Representative flow cytometry contour plots of n- and iTregs in the cLP (gate: Live, CD45+ CD3+ CD4+) (n = 3–8).

Each symbol represents an individual mouse. Data are from one experiment representative of four independent experiments and presented as mean ± SEM. ns, not significant: *p < 0.05, **p < 0.01, ***p < 0.005 by two-way ANOVA with Tukey's multiple comparisons test.

lymphadenopathy, and a reduction in the percentage of CD45+ immune cells migrating to the cLP, although THC did not reduce total immune cell numbers (Figures 4A and 4B). αCD40 injection resulted in an acute release of IL-22 that, counterintuitive to the protective role of IL-22 in infection and chemical models (Gronke et al., 2019; Manta et al., 2013), is pathogenic at these levels (Eken et al., 2014). THC reduced the secretion of IL-22 from cLP cells in αCD40 mice (Figure 4C). Given that a screen of cytokine activity from the serum at day 3 (Figure 3B) revealed no increase in anti-inflammatory cytokines IL-4, IL-10, or IL-9 after THC treatment, we considered mechanisms for αCD40 suppression independent of Th2 cytokines. We examined cLP APCs and found that THC reduced cLP CD11b+ F4/80+ macrophages but did not alter cLP MHCII$^{HI}$CD11c+ DCs (gating strategies are detailed in Figures S1A–S1D) (Figures 4D and 4E). Despite a reduction in cLP macrophages seen with THC treatment, activation markers CD80 and CD86 were unchanged in αCD40 mice given THC, but DC CD80 expression was reduced with THC (Figure S2A–S2D). To assess how cLP DCs played a role in disease, we characterized the subsets of DCs known to heavily influence intestinal inflammatory balance. We phenotyped DCs for their expression of surface markers CD103 and CD11b, because DCs with higher expression of CD103 have been shown to play a role in promoting an anti-inflammatory response through Treg induction (Coombes et al., 2007), whereas DCs with more CD11b expression are catalysts for T cell and ILC inflammatory responses (Persson et al., 2013). THC treatment caused an increase in CD103+ DCs and a concurrent decrease in CD103+ CD11b + DCs at sacrifice compared with VEH mice (Figure 4F). Natural FoxP3+Helios + Tregs were increased with αCD40 compared with IgG, and THC added to that effect compared with VEH (Figure 4G). In the mLN, THC treatment reduced IFNγ-secreting CD8+ CTL and CD4+ Th1 cells compared with VEH (Figures S2E–S2H), whereas there were no observed differences in CD4+ IL-17A-, IL-10-, or IL-4-secreting cells or in DC phenotype (Figures S2G–S2L).

## CB2 Activation on Dendritic Cells Reduces Activation Markers and Increases TGF-β1 Production

A THC-mediated change in DC phenotype was also observed in chemical models of colitis induced by picrylsulfonic acid solution (TNBS) and DSS (Figures S3A and S3B), thus to see the role DCs played in THC colitis protection, naive mice were used. WT mice were given a single administration (1X) of VEH or THC, and 24 h later cLP DCs were analyzed, revealing that THC increased DC CD103 expression and reduced CD11b expression under basal conditions (Figure 5A). Using WT, Cnr1$^{-/-}$ and Cnr2$^{-/-}$ mice, THC increased CD103 expression in all genotypes of mice; however, naive Cnr2$^{-/-}$ had reduced overall levels of cLP DCs compared with WT and Cnr1$^{-/-}$ mice (Figure S4A). Concordantly, we noticed a CB2-dependent increase in FoxP3+ Helios+ nTregs after THC administration (Figure 5B). Upregulation of chemokine receptor 7 (CCR7) is important for the trafficking of DCs between lymph tissues (Schulz et al., 2009) and has been reported to be one mechanism through which DCs can initiate Tregs in the cLP. DCs in the mLNs and cLP of mice given 1X THC had reduced CCR7 expression compared with VEH controls (Figure 5C). Another mechanism through which CD103+ DCs can influence Treg induction is through TGF-β1 secretion (Coombes et al., 2007), and supernatants recovered from cLP cells harvested from THC or VEH 1X mice and plated overnight revealed increased total TGF-β1 production in the THC-treated mice (Figure 5D). Neither was the increase in CD103+ DCs seen in the cLP after acute THC administration noticed in the mLN of these mice (Figure S4B) nor was an increase in mLN total TGF-β1 production seen (Figure S4C). To isolate the effects of THC on DCs specifically, bone-marrow dendritic cells (BMDCs) were generated by addition of GM-CSF and IL-4 to a culture of naive BM cells. VEH or THC was added *in vitro* at the time of polarization, and each time media was changed to reveal that at the end of culture the THC-treated BMDCs had more total TGF-β1 in their supernatant (Figure 5E). Although there were equivalent percentages of DCs in the VEH- and THC-treated cultures, a BMDC culture is a mixed population of cells, so on day 6 of BMDC culture, CD11c+ DCs were purified and plated overnight without extra VEH or THC, their supernatant

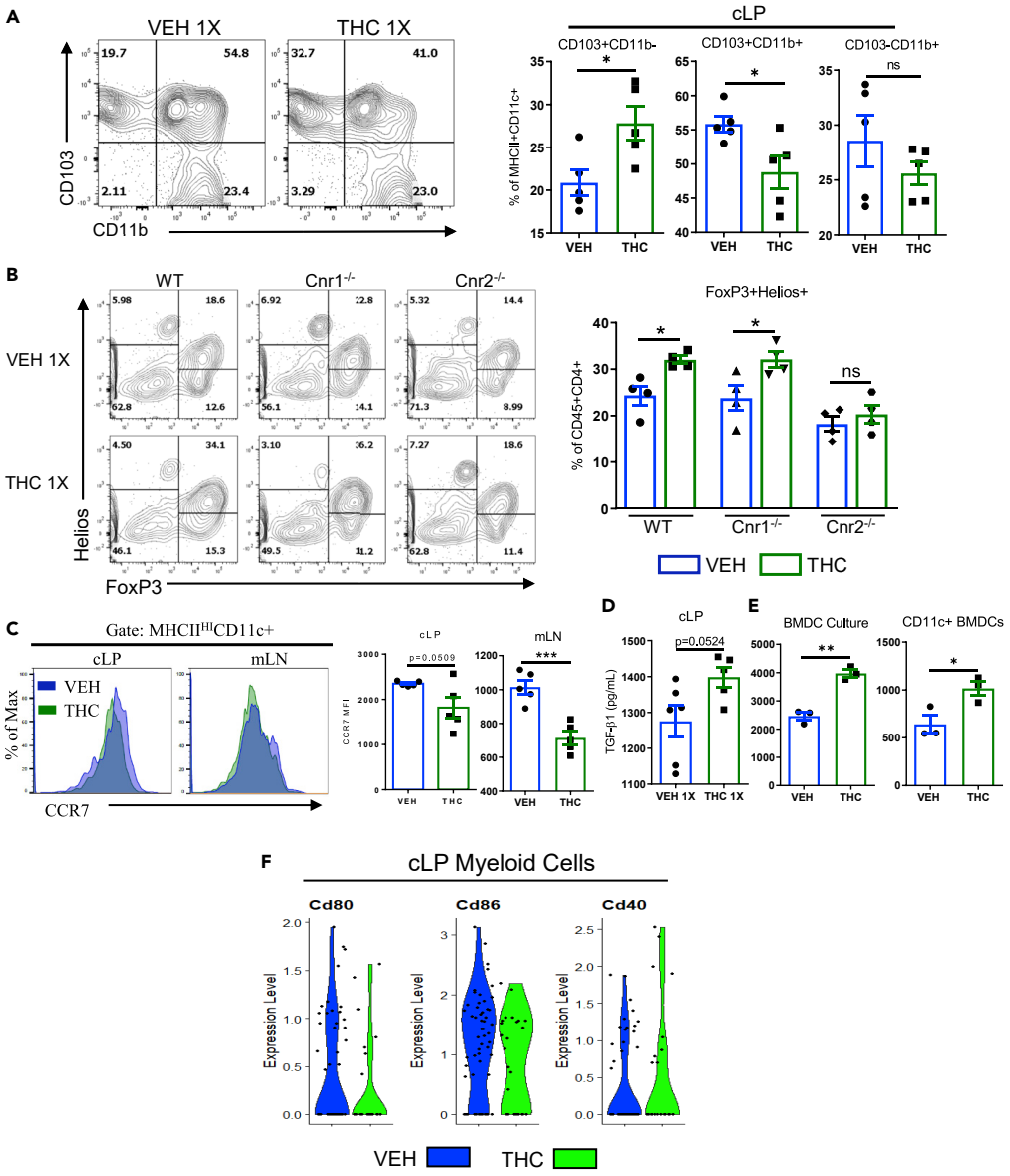


**Figure 5. CB2 Activation on Dendritic Cells Reduces Activation Markers and Increases TGF-β1 Production**

Naive mice were administered VEH or THC (10 mg/kg) once, and 24 h later cLP and mLN were harvested.

(A) Representative flow cytometry contour plots of dendritic cell subsets in the cLP.

(B) Flow cytometry contour plots displaying FoxP3+ Helios+ nTregs and FoxP3+ Helios- iTregs (gate: Live, CD45+ CD4+) (n = 4).

(C) Representative flow cytometry-overlaid histograms and median fluorescence intensity (MFI) of CCR7 expression in DCs from indicated mice in the cLP or mLN (n = 5).

(D and E) (D) Total TGF-β1 levels from the supernatants of cLP cells deriving from mice treated with VEH or THC for 24 h (n = 5–6) and (E) BMDCs treated with VEH or THC after 7 days of culture with treatment, or after 1 day of culture after CD11c+ cell selection (n = 3). Each symbol represents an individual mouse. Data are from one experiment representative of two independent experiments and presented as mean ± SEM. NS, not significant: *p < 0.05, **p < 0.01, ***p < 0.005 by two-way ANOVA with Tukey's multiple comparisons test.

(F) scRNA-seq violin plot of indicated mRNA expression in the myeloid cell cluster from the colon of mice treated with VEH or THC for 24 h.

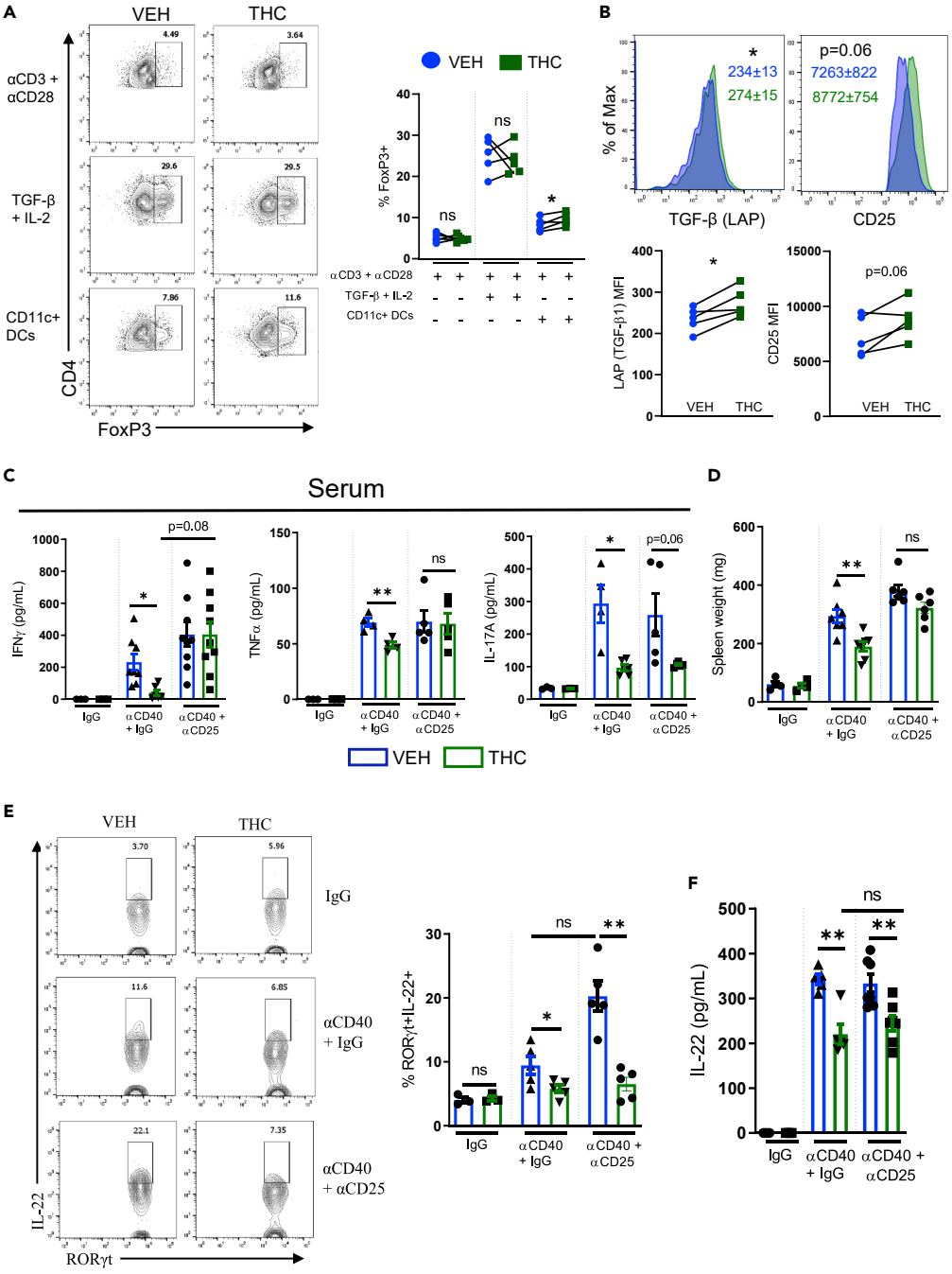


**Figure 6. THC Induces Tregs through DCs to Reduce Systemic but Not Colonic Inflammation**

Lymph nodes and spleens were harvested from naive mice, and CD4+ T cells and CD11c+ APCs were selected via magnetic bead purification. Purified CD4+ T cells were plated for 5 days under conditions of T cell stimulation: (αCD3 + αCD28), Treg polarization: (αCD3 + αCD28 + IL-2 + TGF-β1), or with purified CD11c+ cells at a ratio of 5:1, CD4+:CD11c+, and then samples from individual mice were treated with either VEH or THC (10 μM).

(A) Flow cytometry contour plots and quantification of CD4+ FoxP3+ Tregs (gate: Live, CD4+) after 5 days of culture under indicated conditions (n = 5).

(B) Representative overlaid histograms of indicated markers from THC- or VEH-treated CD4+ T cells after Treg polarization (gate: Live, CD4+ FoxP3+) (n = 5). Each symbol represents a paired comparison from a single mouse whose cells were split up into VEH or THC treatment. Data are from one experiment representative of two independent experiments and presented as mean ± SEM. NS, not significant: *p < 0.05, **p < 0.01 by Student's t test. 10 days before disease induction Treg were depleted via i.p. injection of rat anti-mouse CD25 (clone PC61, 250 μg/mouse) or isotype

**Figure 6. *Continued***
control. Mice were pre-treated with VEH or THC (10 mg/kg) for 2 days before disease induction by i.p. injection of αCD40 or IgG control.
(C) ELISA for serum cytokines IFNγ, TNFα, and IL-17A (n = 3–6).
(D) Spleen weights at end of experiment (n = 3–6).
(E) Representative flow cytometry contour plots and quantification of IL-22-secreting ILC3s (gate: Live, Lineage- $CD45^{INT}CD90.2^{HI}$CD3- RORγt+) (n = 3–6).
(F) ELISA results for IL-22 from cLP supernatants recovered from indicated mice on day 7 (n = 3–5).
Each symbol represents an individual mouse. Data are presented as mean ± SEM from one experiment that was repeated 3 times. NS, not significant: *p < 0.05, **p < 0.01 by two-way ANOVA with Tukey's multiple comparisons test.

recovered, and total TGF-β1 levels were analyzed and increased from the THC-treated BMDCs compared with VEH controls (Figure 5E). We observed a decrease in DC CD86, but not CD80 expression in THC-treated cultures; THC-treated DCs reduced CD4 and CD8 T cell proliferation *in vitro* (Figures S4D and S4E). We confirmed these results in naive mice through single-cell RNA sequencing (scRNA-seq) of colonic cells 24 h after VEH or THC administration (Figure S3C). scRNA-seq allowed for the isolation of myeloid cells from other cell types, revealing that THC decreases myeloid cell expression of *Cd80* and *Cd86*, but increased expression of *Cd40* (Figure 5F).

## THC Induces Tregs through DCs to Reduce Systemic but Not Colonic Inflammation

To decipher whether THC acted directly on T cells or through DCs to stimulate Tregs, CD4+ T cells were isolated from naive mice and plated under conditions of T cell stimulation (αCD3 and αCD28), Treg polarization (αCD3, αCD28, IL-2 and TGF-β1), or with CD11c+ APCs, with or without THC. Only when T cells were plated with CD11c+ APCs did THC increase the percentage of Tregs (Figure 6A); however, THC acted directly on polarized Tregs to increase the surface expression of functional markers TGF-β1 (LAP) and CD25 (Figure 6B), but GARP, ICOS, and CD223 (LAG-3) were unchanged (Figure S4F).

To assess the role Tregs play in THC's attenuation of αCD40 inflammatory processes, Tregs were depleted from mice via i.p. injection of anti-CD25, which has been shown to reduce Tregs 8 days after a single injection (Setiady et al., 2010), and were absent in the mLN of anti-CD25-treated mice, but not in IgG control or αCD40+ IgG-treated mice (Figure S5B). Treatment with THC or VEH began 5 days after anti-CD25 or IgG administration and 2 days before αCD40. Neither did Treg-depleted mice given αCD40 exhibit greater loss of body weight compared with αCD40+ IgG mice nor did THC alter wasting (Figure S5A). THC reduced serum IFNγ and TNFα only in αCD40+ IgG mice, not in Treg-depleted αCD40 mice; Treg depletion did not change THC's ability to reduce serum IL-17A induced by αCD40 (Figure 6C). Loss of Tregs prevented the reduction in spleen weight seen with THC+ αCD40 IgG (Figure 6D). Colitogenic ILC3 production of IL-22 in the αCD40 model is in part regulated by Tregs (Bauché et al., 2018); however, our results indicate that THC reduces IL-22-secreting ILC3s as well as total colonic production of IL-22 independently of Tregs (Figures 6E and 6F).

## THC Reduces Colonic APC Activation Markers through Cannabinoid Receptors

As we showed that Tregs induced by THC are not the intermediary preventing colonic inflammation, we sought to analyze the other immune cell changes that occur after acute THC administration under naive conditions. We found that neither does THC affect the percent of ILCs: ILC2, NCR, or LTi ILC3s in the cLP, nor are macrophage numbers changed, although there is an increase in FCεRI+ c-Kit+ mast cells in the cLP after THC administration, and this is mediated through CB2 (Figures S5C and S5D). THC1X-treated mice whose cLP was isolated and plated overnight only show small differences by an increase in IL-2 and IL-6 production compared with VEH-treated mice (Figure S5E). In consideration of the global reduction in pro-inflammatory cytokines seen with THC after αCD40 administration, we looked at myeloid cells in various tissues to look at how THC affects their immunogenicity. The cLP, mLN, spleen, lung, liver, and brain of naive WT, $Cnr1^{-/-}$, and $Cnr2^{-/-}$ mice were removed, brought to a single-cell suspension, and plated overnight in the presence of VEH or THC (10μM) and then analyzed by flow cytometry for APC activation markers of interest: CD40, CD80, CD86, Ly-6C, Ly-6G, CD103, CX3CR1, and MHCII. Heatmaps display median fluorescence intensity (MFI) for each marker of interest gated on either macrophages (Macs) or DCs from that tissue (gating strategies for individual tissues are in Figures S1A–S1D) (Figure 7A). The heatmaps are normalized per row such that increased MFI of highly expressed markers (e.g., MHCII on DCs) does not overshadow the differences in markers with lower expression. Only markers that displayed significant differences with THC treatment are displayed graphically. We found that in the colonic lymph tissue, THC

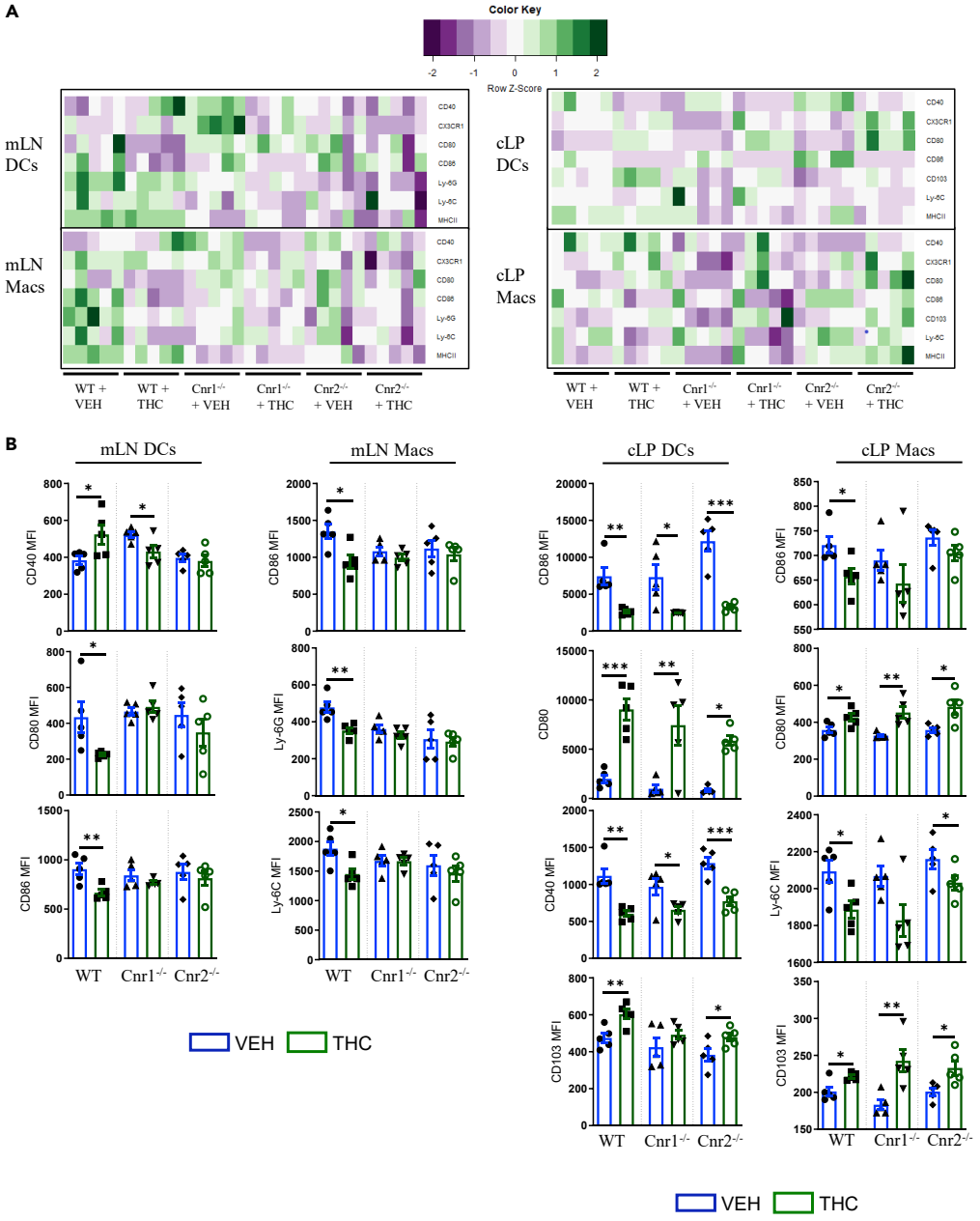


**Figure 7. THC Reduces APC Activation Markers through Cannabinoid Receptors**

Naive age and sex-matched WT, Cnr1$^{-/-}$, and Cnr2$^{-/-}$ mice were euthanized and colonic lamina propria (cLP), mesenteric lymph nodes (mLNs), spleens (spl), livers, lungs, and brain were brought to a single-cell suspension and then treated *ex vivo* with either VEH or THC (10 μM) for 18 h before being analyzed for markers of antigen-presenting cell (APC) activation by flow cytometry.

(A) Heatmap of median fluorescence intensities of (in descending order) CD40, CX3CR1, CD80, CD86, Ly-6G, Ly-6C, and MHCII on macrophages and dendritic cells from tissues deriving from WT, Cnr1$^{-/-}$, or Cnr2$^{-/-}$ mice treated with VEH or THC. Heatmap intensity was normalized per row/marker of interest.

(B) Quantification of flow cytometry results (n = 5).

Each symbol represents a different mouse. Data are from one experiment representative of two independent experiments and presented as mean ± SEM. *p < 0.05, **p < 0.01, ***p < 0.005 by two-way ANOVA with Tukey's multiple comparisons test.

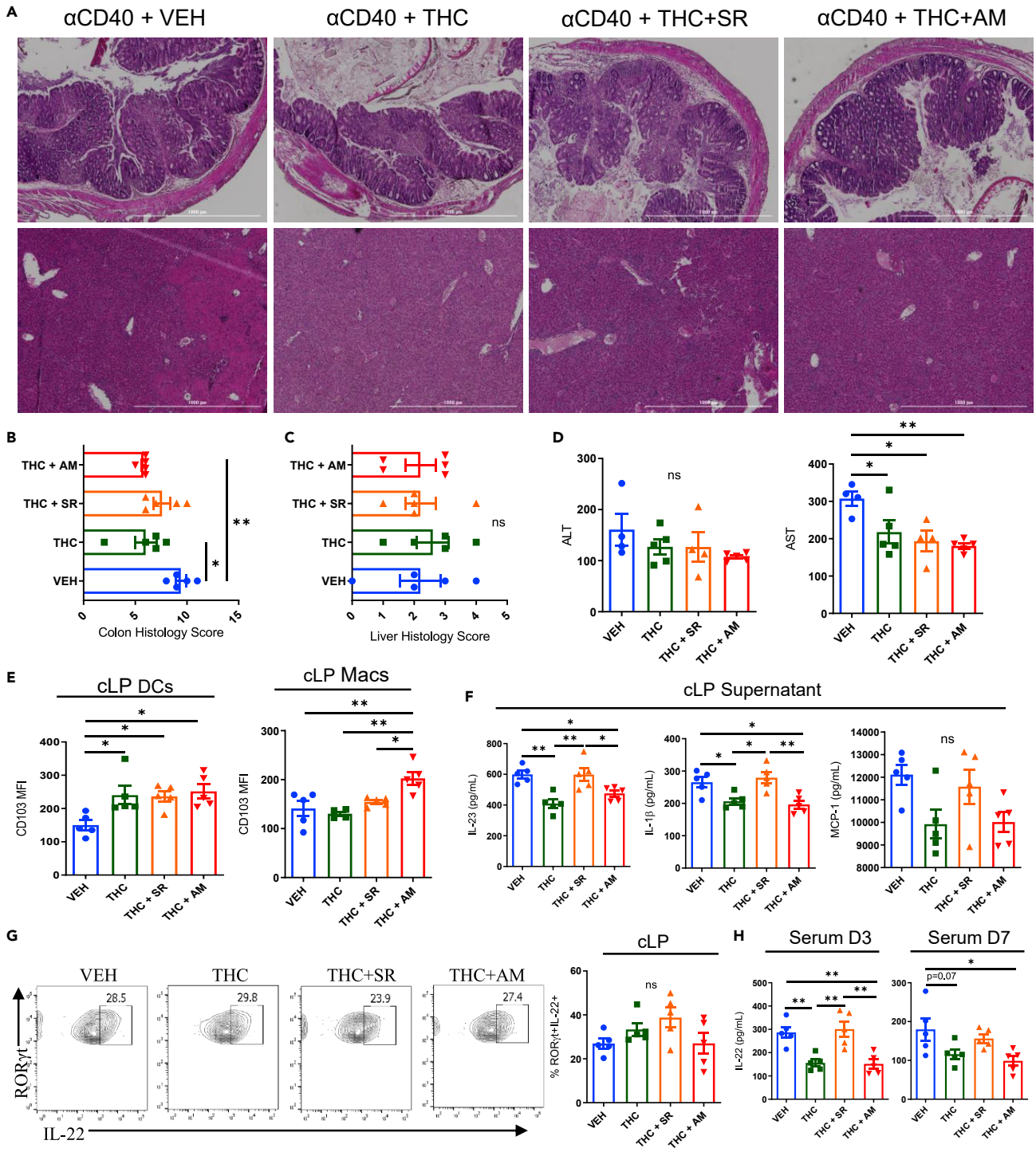


**Figure 8. Cannabinoid Receptor 2 Activation on Myeloid Cells Mediates Colonic Resistance to αCD40-Induced Inflammation**

SCID mice were injected with rat anti-mouse αCD40 (200 μg, clone FGK4.5 in PBS) and received VEH, THC (10 mg/kg), THC+ SR144528 (THC+ SR, 10 mg/kg, both), or THC+ AM251 (THC + AM, 10 mg/kg, both) daily for 7 days.

(A) Representative H&E images of colons (upper row, 4X) and livers (lower row, 4X) from indicated mice.

(B and C) (B) Histological scoring of colon and (C) liver H&E images (n = 5).

(D) ALT and AST activities were measured from the serum of indicated mice at termination of the experiment (n = 5).

(E) Median fluorescence intensity of CD103 on DCs and macrophages from the cLP of *SCID* mice given αCD40 and VEH or THC ± CB antagonists (n = 5).

(F) ELISA for cLP supernatant cytokines IL-23, IL-1β, and MCP-1 (n = 5).

**Figure 8. *Continued***

(G) Flow cytometric contour plots of RORγt+ IL-22+ ILC3s in the cLP of indicated mice at termination of the experiment (n = 5).

(H) ELISA for serum cytokine IL-22 at days 3 and 7 (n = 5).

Each symbol represents a different mouse. Data are from one experiment representative of two independent experiments and presented as mean ± SEM. *p < 0.05, **p < 0.01 by two-way ANOVA with Tukey's multiple comparisons test.

reduced DC expression of CD86 in the mLN and cLP, but increased CD80 expression in cLP DCs. Expression of CD40 was increased in the presence of THC in mLN DCs, but decreased with THC in cLP DCs, and CD103 was increased on cLP DCs. In intestinal macrophages, CD86 and Ly-6C expression was reduced on mLN and cLP macrophages, whereas in the cLP, CD80 and CD103 expression was increased on macrophages, as seen in DC (Figure 7B).

In the other tissues examined, there was a trend toward decreased expression of all markers in $Cnr2^{-/-}$ mice compared with WT and $Cnr1^{-/-}$ mice, which was most pronounced among lung DCs (Figures S6A–S6D). Interestingly, neither macrophages nor DCs in the liver showed a change in activation markers with THC (Figure S6A). Similar to in the intestines, lung and spleen DCs showed a decrease in CD86 expression mediated by CB2 in the spleen (Figures S6B and S6C). Ly-6C is reduced with THC in DCs of the lung and microglia, and CX3CR1 is also decreased in these tissues and in spleen macrophages (Figures S6A–S6D). CD40 and Ly-6G are also increased in microglia with THC (Figure S6D). Collectively, THC reduces APC activation markers specifically in the mucosal barrier sites in the intestines and lungs.

### Cannabinoid Receptor 2 Activation on Myeloid Cells in SCID Mice Mediates Colonic Resistance to αCD40-Induced Inflammation

In light of the data on THC's blunting of APC stimulatory capacity, and the fact that Tregs are not the mechanism through which THC reduces colonic IL-22 production, we initiated the αCD40 model in T- and B-cell deficient mice to examine how THC modulation of myeloid cells affects disease course. Like in WT BL/6 mice, T- and B-cell-deficient *SCID* mice given αCD40 undergo acute weight loss, and treatment with VEH, THC, or THC plus CB receptor antagonists AM251 (CB1 antagonist) or SR144528 (CB2 antagonist) did not alter αCD40-induced wasting (Figure S7A). THC and THC + AM reduced colonic inflammation, but not liver necro-inflammation (Figures 8A–8C). No treatments reduced serum ALT activity; however, THC, THC + SR, and THC + AM reduced serum AST activity, which may suggest a reduction in muscle wasting seen with cannabinoids (Figure 8D). Seven days after disease induction, cLP DCs and macrophages were analyzed, confirming that THC, THC + SR, and THC + AM increased DC CD103 expression, as seen in WT mice (Figures 8E and S7B), but on macrophages only CB2 agonism in the THC + AM group increased macrophage expression of CD103 (Figures 8E and S7B). Lamina propria cells were plated overnight and supernatants were collected, revealing that THC and THC + AM treatment reduced IL-23 and IL-1β production, but not MCP-1 levels, although there was a trend toward a decrease (Figure 8F). In naive mice given VEH or THC for 24 h, scRNA-seq data indicated that basal expression of *Il1b* and *Ccl2* (MCP-1) were unchanged between VEH- and THC-treated mice (Figure S7C). In this T-cell-deficient model of αCD40-induced colitis, ILC3s are the main source of colonic IL-22, which was unchanged after any cannabinoid treatment (Figure 8G). Nonetheless, circulating IL-22 was reduced in the THC and THC + AM groups compared with VEH and THC + SR groups at peak of disease and termination of the study (Figure 8H).

## DISCUSSION

Developing colitis is multi-factorial and arises as the result of an imbalance between the host barrier, immune cells, and commensals (Lynch and Pedersen, 2016). Recent evidence suggests that IBD is increasing globally (Coward et al., 2019; Kaplan and Ng, 2016), and as genetics is unlikely to be the culprit given the timescale, we must consider the interactions between the environment, commensals, and our immune cells' response to them, as disease instigating. Modulation of gut interactions between any of the actors can tip the scales toward either promotion or protection from IBD. Many studies have shown that cannabinoids exhibit potential in tipping that scale toward tolerance to protect against IBD (Singh et al., 2012; Storr et al., 2009; Ke et al., 2016; Kimball et al., 2006). However, data on the anti-colitic effects of cannabinoids in humans does not recapitulate what is seen in mouse models (Ambrose and Simmons, 2019; Naftali et al., 2013; Lahat et al., 2012). In the AOM + DSS model of CRC, THC treatment prevented cancer development and reduced pro-tumorigenic intra-epithelial-infiltrating IL-22-producing Th22 cells. IL-22 has gained attention for its carcinogenic properties in human patients and in animal models of colon cancer by promoting cancer stemness through STAT-3 activation (Sun et al., 2015; Kryczek et al., 2014; Kirchberger

et al., 2013). Our results demonstrated that THC attenuated tumorigenic IL-22 in the colonocyte microenvironment acting through CB2 on hematopoietic cells; however, this effect was not Th22 intrinsic, because THC did not directly affect the isolated generation of Th22 cells *in vitro*. The stimulation of both Th22 and ILC3s to produce IL-22 is regulated by pro-inflammatory cytokines such as IL-1β, IL-6, MCP-1, and IL-23 from local APCs (Parks et al., 2016; Manta et al., 2013; Dudakov et al., 2015). Thus, we used the anti-CD40 model of colitis in WT and in T- and B-cell-deficient mice to investigate how THC can act on the adaptive and innate immune system to reduce IL-22 in a model where it is pathogenic to the proximal colon, independent of the microbiota, and does not rely on exogenous chemicals to mediate disease progression (Uhlig et al., 2006).

Injection of anti-CD40 causes acute wasting disease and colitis dependent on secretion of inflammatory cytokines TNFα, IL-12, and IL-23 (Eken et al., 2014; Longman et al., 2014; Uhlig et al., 2006). We found in the anti-CD40 colitis model that THC reduced systemic and colonic inflammation via reduction in gross intestinal pathology and circulating pro-inflammatory cytokines IFNγ, TNFα, IL-17A, and IL-22. Systemic inflammation induced by anti-CD40 was reduced with THC as measured by a reduction in splenomegaly and biomarkers for liver damage AST and ALT. THC treatment in anti-CD40 mice resulted in an increase in Tregs in the cLP that was mediated by THC working directly on DCs to increase CD103 expression and reduce CD11b expression, converting them into more tolerogenic cells with increased TGF-β1 expression confirmed by scRNA-seq. Acting through CB2, we demonstrated that THC modulates cLP DC phenotype toward a more anti-inflammatory state, characterized by decreased expression of CD80 and CD11b in anti-CD40 colitic mice *in vivo*. Our scRNA-seq data of cLP myeloid cells, and *ex vivo* flow cytometric analysis of naive bone-marrow derived DCs and DCs deriving from the cLP, mLN, spleen, and lung, all showed a reduction in CD86 expression with THC. An interesting finding from our flow cytometric analysis of global APC activation markers revealed that whereas THC polarized DCs toward a more tolerogenic phenotype with increased CD103 expression and reduced CD86 expression, THC also acted on mLN DCs and microglia to increase CD40 expression. Increased CD40 signals on CD103+ DCs to upregulate CCR7, causing them to move to the mLN and apoptose (Barthels et al., 2017). Given that we have seen THC reduce CCR7 expression in the cLP and mLN, that is unlikely to be causing DC apoptosis; however, CD40 acts with previously antigen-activated CD40L+ T cells to co-stimulate in a positive feedback loop when they have encountered familiar antigens (Cong et al., 2000). THC upregulation of CD40 in the mLN but downregulation of other activation markers suggested that THC may prime intestinal immunity for identified antigens, but reduce its effectiveness at stimulating an immune response to novel antigens in the cLP, which could explain why cannabinoids are ineffective at clearing infection models of colitis but are effective in chemical models (Eisenstein and Meissler, 2015; Newton et al., 2009; Karmaus et al., 2011). THC upregulation of CD40 could similarly be a compensatory mechanism to account for the downregulation of CD80 and CD86.

DCs in the cLP can promote the expansion of T regulatory cells. Several studies have examined this mechanism, suggesting that DCs, primarily CD103+ DCs, upregulate CCR7 to migrate to the mLN where they secrete TGF-β1 and retinoic acid to induce T regulatory cells (Schulz et al., 2009). Our results showed that THC administration in naive mice and after anti-CD40-induced colitis caused a decrease in CCR7 expression on DCs in both the cLP and mLN, suggesting that THC reduces DC migration between gastrointestinal lymph tissue. In addition, we found that BMDCs treated with THC and cells from the cLP of mice treated with THC exhibited increased levels of TGF-β1. Taken together these data indicate that in the intestines, THC causes DCs to, instead of migrating to the mLN and induce Tregs, remain in the cLP, downregulate activation marker CD86, secrete TGF-β1, and increase the percentage of Tregs and influence other local cell types through the anti-inflammatory actions of TGF-β1. TGF-β1 is critical for intestinal homeostasis. Global TGF-β1$^{-/-}$ mice develop spontaneous colitis around 3–4 weeks of age, and DC-specific knockout of TGF-β1 results in spontaneous colitis (Ihara et al., 2017; Ramalingam et al., 2012). DCs are an important source and activator of TGF-β1 in the intestine, necessary for controlling Treg and Th17 differentiation (Ramalingam et al., 2012) and colonocyte homeostasis (Ihara et al., 2016). The effect of THC on DCs follows the observation that THC treatment reduces APC activity in mice (Karmaus et al., 2011) and *in vitro* in human cells (Roth et al., 2015). To examine the THC-mediated cellular contributions to a reduction in anti-CD40 severity, we first depleted Tregs via injection of anti-CD25, revealing that THC's reduction in systemic inflammation caused by anti-CD40 is in part mediated by Tregs, because in mice depleted of Tregs given THC, circulating IFNγ and TNFα were increased back to control levels and splenomegaly was not reduced. A study done in *Rag2*$^{-/-}$ mice found that adoptively transferring Tregs did not alter systemic inflammation (Bauché et al., 2018); however, the metric they used to conclude that was body weight, which was also unchanged in our study with THC, with or without Tregs, although circulating biomarkers of disease activity and spleen weight were changed. Nevertheless, anti-CD40-induced colonic inflammation in WT mice is not

ameliorated by THC-induced Tregs, as depleting Tregs did not dampen THC's reduction in IL-17A or ILC3 secretion of IL-22. Cytokine data also revealed that THC did not increase other Th subset anti-inflammatory cytokines IL-4, IL-10, or IL-9, suggesting that THC's salutary capabilities lied in its modulation of APCs.

Data from T- and B-cell-deficient *SCID* mice injected with anti-CD40 reinforced what was seen in WT mice—APCs from the colon are stimulated by anti-CD40 to induce pro-inflammatory IL-23 and IL-1β, which are both reduced with CB2 agonism, and MCP-1, which displayed a non-significant decreasing trend with THC and THC + AM251 treatment. scRNA-seq analysis of WT cLP myeloid cells showed a similar decrease in *Il1b* and *Ccl2* after THC treatment. The decrease in colonic inflammation in *SCID* αCD40 mice was not mirrored by a decrease in systemic inflammation as assessed by liver pathology and ALT levels, reinforcing what we observed in Treg-depleting studies in WT mice. THC and a combination of THC and both antagonists reduced circulating AST levels, suggesting that THC may reduce muscle wasting in this model, either through a CB redundant effect or through GPR55. The main finding from this experiment was that THC acted on both sentinel APCs in the colon, DCs, and macrophages, to increase CD103 and decrease pro-inflammatory mediators that stimulate IL-22 production. Although our cLP data do not display differences in ILC3 secretion, IL-22 levels in the serum are significantly decreased at both days 3 and 7 with THC and THC + AM treatment, confirming the role of CB2 in reducing IL-22 secretion.

In this study, we demonstrate that THC agonism of CB2 is the mechanism through which intestinal APCs undergo a phenotypic switch toward a more anti-inflammatory phenotype characterized by increased expression of CD103 and decreased CD86. These APCs are less primed to secrete the pro-inflammatory mediators IL-23, IL-1β, and MCP-1, instead increasing TGF-β1 to induce Tregs in the local microenvironment. Tregs are important to resolve αCD40-induced inflammation systemically, able to reduce liver inflammation and splenomegaly; however, in the colon, it is through THC's actions on DCs and macrophages that THC can reduce pathogenic levels of IL-22 to protect the host from undue inflammation and cancer. Here we have dissected how CB2 activation can refine myeloid cell phenotype to abrogate inflammation and prevent colitis and developing colon cancer.

### Limitations of the Study

Using a *de novo* tumor model and models of chemically induced and antibody-induced colitis, this study delineates the mechanisms through which THC, acting through CB2 on gut APCs, limits the secretion of pro-inflammatory cytokines that would otherwise go on to stimulate oncogenic Th22 and ILC3 release of IL-22. Determining if a reduction in IL-22 in THC-treated mice is the sole actor preventing the development of CRC will be illuminating and worthwhile to evaluate in future work. Although this study evaluated the cancer-preventative action of THC, studies evaluating the effect of THC on developed tumors would be clinically relevant.

### Resource Availability

#### *Lead Contact*

Further information and requests for resources and reagents should be directed to and will be fulfilled by the Lead Contact, Prakash S. Nagarkatti, Ph.D (prakash@Mailbox.Sc.Edu).

#### *Materials Availability*

This study did not generate new unique reagents.

#### *Data and Code Availability*

Raw sequencing data is available at the Sequence Read Archive (SRA) accession: PRJNA592156, and processed data files are available at Gene Expression Omnibus (GEO) accession number: GSE155669.

## METHODS

All methods can be found in the accompanying Transparent Methods supplemental file.

## SUPPLEMENTAL INFORMATION

Supplemental Information can be found online at https://doi.org/10.1016/j.isci.2020.101504.

## ACKNOWLEDGMENTS

These studies were supported in part by NIH grants: P01AT003961, P20GM103641, R01AT006888, R01ES030144, and R01AI123947.

## AUTHOR CONTRIBUTIONS

Designed Research Studies, W.B., H.R.A., M.N., and P.S.N.; Experimentation and Data Acquisition, W.B., H.R.A., K.M., and C.C.; Data Analysis, W.B., K.W., G.C., I.C., and H.R.A.; Writing – Original Manuscript Draft, W.B.; Writing – Editing and Revisions, W.B., M.N. and P.S.N.; Funding Acquisition, M.N. and P.S.N.; Resources, M.N. and P.S.N.; Supervision, M.N. and P.S.N.

## DECLARATION OF INTERESTS

The authors have declared that no conflicts of interest exist.

Received: May 29, 2020
Revised: July 20, 2020
Accepted: August 24, 2020
Published: September 25, 2020

## REFERENCES

Ambrose, T., and Simmons, A. (2019). Cannabis, cannabinoids, and the endocannabinoid system-is there therapeutic potential for inflammatory bowel disease? J. Crohns Colitis *13*, 525–535.

Brand, S., Beigel, F., Olszak, T., Zitzmann, K., Eichhorst, S.T., Otte, J.M., Diepolder, H., Marquardt, A., Jagla, W., Popp, A., et al. (2006). IL-22 is increased in active Crohn's disease and promotes proinflammatory gene expression and intestinal epithelial cell migration. Am. J. Physiol. Gastrointest. Liver Physiol. *290*, G827–G838.

Bauché, D., Joyce-Shaikh, B., Jain, R., Grein, J., Ku, K.S., Blumenschein, W.M., Ganal-Vonarburg, S.C., Wilson, D.C., McClanahan, T.K., Malefyt, R.d.W., et al. (2018). LAG3+ regulatory T cells restrain interleukin-23-producing CX3CR1+ gut-resident macrophages during group 3 innate lymphoid cell-driven colitis. Immunity *49*, 342–352.e5.

Barthels, C., Ogrinc, A., Steyer, V., Meier, S., Simon, F., Wimmer, M., Blutke, A., Straub, T., Strobl, U.Z., Lutgens, E., et al. (2017). CD40-signalling abrogates induction of RORγt+ Treg cells by intestinal CD103+ DCs and causes fatal colitis. Nat. Commun. *8*, 14715.

Coward, S., Clement, F., Benchimol, E.I., Bernstein, C.N., Avina-Zubieta, J.A., Bitton, A., Carroll, M.W., Hazlewood, G., Jacobson, K., Jelinski, S., et al. (2019). Past and future burden of inflammatory bowel diseases based on modeling of population-based data. Gastroenterology *156*, 1345–1353.e4.

Cianchi, F., Papucci, L., Schiavone, N., Lulli, M., Magnelli, L., Vinci, M.C., Messerini, L., Manera, C., Ronconi, E., Romagnani, P., et al. (2008). Cannabinoid receptor activation induces apoptosis through tumor necrosis factor alpha-mediated ceramide de novo synthesis in colon cancer cells. Clin. Cancer Res. *14*, 7691–7700.

Coombes, J.L., Siddiqui, K.R., Arancibia-Cárcamo, C.V., Hall, J., Sun, C.M., Belkaid, Y., and Powrie, F. (2007). A functionally specialized population of mucosal CD103+ DCs induces Foxp3+ regulatory T cells via a TGF-beta and retinoic acid-dependent mechanism. J. Exp. Med. *204*, 1757–1764.

Cho, J.H. (2008). The genetics and immunopathogenesis of inflammatory bowel disease. Nat. Rev. Immunol. *8*, 458–466.

Cong, Y., Weaver, C.T., Lazenby, A., and Elson, C.O. (2000). Colitis induced by enteric bacterial antigen-specific CD4+ T cells requires CD40-CD40 ligand interactions for a sustained increase in mucosal IL-12. J. Immunol. *165*, 2173–2182.

Dyson, J.K., and Rutter, M.D. (2012). Colorectal cancer in inflammatory bowel disease: what is the real magnitude of the risk? World J. Gastroenterol. *18*, 3839–3848.

De Jong, Y.P., Comiskey, M., Kalled, S.L., Mizoguchi, E., Flavell, R.A., Bhan, A.K., and Terhorst, C. (2000). Chronic murine colitis is dependent on the CD154/CD40 pathway and can be attenuated by anti-CD154 administration. Gastroenterology *119*, 715–723.

Dudakov, J.A., Hanash, A.M., and van den Brink, M.R. (2015). Interleukin-22: immunobiology and pathology. Annu. Rev. Immunol. *33*, 747–785.

Duerr, R.H., Taylor, K.D., Brant, S.R., Rioux, J.D., Silverberg, M.S., Daly, M.J., Steinhart, A.H., Abraham, C., Regueiro, M., Griffiths, A., et al. (2006). A genome-wide association study identifies IL23R as an inflammatory bowel disease gene. Science *314*, 1461–1463.

de Souza, H.S.P., and Fiocchi, C. (2016). Immunopathogenesis of IBD: current state of the art. Nat. Rev. Gastroenterol. Hepatol. *13*, 13–27.

Eken, A., Singh, A.K., Treuting, P.M., and Oukka, M. (2014). IL-23R+ innate lymphoid cells induce colitis via interleukin-22-dependent mechanism. Mucosal Immunol. *7*, 143–154.

Eisenstein, T.K., and Meissler, J.J. (2015). Effects of cannabinoids on T-cell function and resistance to infection. J. Neuroimmune Pharmacol. *10*, 204–216.

Fujino, S., Andoh, A., Bamba, S., Ogawa, A., Hata, K., Araki, Y., Bamba, T., and Fujiyama, Y. (2003). Increased expression of interleukin 17 in inflammatory bowel disease. Gut *52*, 65–70.

Gronke, K., Hernández, P.P., Zimmermann, J., Klose, C.S.N., Kofoed-Branzk, M., Guendel, F., Witkowski, M., Tizian, C., Amann, L., Schumacher, F., et al. (2019). Interleukin-22 protects intestinal stem cells against genotoxic stress. Nature *566*, 249–253.

Hildner, K., Edelson, B.T., Purtha, W.E., Diamond, M., Matsushita, H., Kohyama, M., Calderon, B., Schraml, B.U., Unanue, E.R., Diamond, M.S., et al. (2008). Batf3 deficiency reveals a critical role for CD8alpha+ dendritic cells in cytotoxic T cell immunity. Science *322*, 1097–1100.

Huang, H., Fang, M., Jostins, L., Umićević Mirkov, M., Boucher, G., Anderson, C.A., Andersen, V., Cleynen, I., Cortes, A., Crins, F., et al. (2017). Fine-mapping inflammatory bowel disease loci to single-variant resolution. Nature *547*, 173–178.

Izzo, A.A., Aviello, G., Petrosino, S., Orlando, P., Marsicano, G., Lutz, B., Borrelli, F., Capasso, R., Nigam, S., Capasso, F., and Di Marzo, V. (2008). Increased endocannabinoid levels reduce the development of precancerous lesions in the mouse colon. J. Mol. Med. *86*, 89–98.

Ihara, S., Hirata, Y., and Koike, K. (2017). TGF-β in inflammatory bowel disease: a key regulator of immune cells, epithelium, and the intestinal microbiota. J. Gastroenterol. *52*, 777–787.

Ihara, S., Hirata, Y., Serizawa, T., Suzuki, N., Sakitani, K., Kinoshita, H., Hayakawa, Y., Nakagawa, H., Ijichi, H., Tateishi, K., and Koike, K. (2016). TGF-β signaling in dendritic cells governs colonic homeostasis by controlling epithelial differentiation and the luminal microbiota. J. Immunol. *196*, 4603–4613.

Kryczek, I., Lin, Y., Nagarsheth, N., Peng, D., Zhao, L., Zhao, E., Vatan, L., Szeliga, W., Dou, Y., Owens, S., et al. (2014). IL-22+CD4+ T cells promote colorectal cancer stemness via STAT3 transcription factor activation and induction of

the methyltransferase DOT1L. Immunity *40*, 772–784.

Kirchberger, S., Royston, D.J., Boulard, O., Thornton, E., Franchini, F., Szabady, R.L., Harrison, O., and Powrie, F. (2013). Innate lymphoid cells sustain colon cancer through production of interleukin-22 in a mouse model. J. Exp. Med. *210*, 917–931.

Kiss, E.A., and Diefenbach, A. (2012). Role of the aryl hydrocarbon receptor in controlling maintenance and functional programs of RORγt+ innate lymphoid cells and intraepithelial lymphocytes. Front. Immunol. *3*, 124.

Karmaus, P.W., Chen, W., Crawford, R.B., Harkema, J.R., Kaplan, B.L., and Kaminski, N.E. (2011). Deletion of cannabinoid receptors 1 and 2 exacerbates APC function to increase inflammation and cellular immunity during influenza infection. J. Leukoc. Biol. *90*, 983–995.

Ke, P., Shao, B.Z., Xu, Z.Q., Wei, W., Han, B.Z., Chen, X.W., Su, D.F., and Liu, C. (2016). Activation of cannabinoid receptor 2 ameliorates DSS-induced colitis through inhibiting NLRP3 inflammasome in macrophages. PLoS one *11*, e0155076.

Kimball, E.S., Schneider, C.R., Wallace, N.H., and Hornby, P.J. (2006). Agonists of cannabinoid receptor 1 and 2 inhibit experimental colitis induced by oil of mustard and by dextran sulfate sodium. Am. J. Physiol. Gastrointest. Liver Physiol. *291*, G364–G371.

Kaplan, G.G., and Ng, S.C. (2016). Globalisation of inflammatory bowel disease: perspectives from the evolution of inflammatory bowel disease in the UK and China. Lancet Gastroenterol. Hepatol. *1*, 307–569.

Lynch, S.V., and Pedersen, O. (2016). The human intestinal microbiome in health and disease. N. Engl. J. Med. *375*, 2369–2379.

Lahat, A., Lang, A., and Ben-Horin, S. (2012). Impact of cannabis treatment on the quality of life, weight and clinical disease activity in inflammatory bowel disease patients: a pilot prospective study. Digestion *85*, 1–8.

Longman, R.S., Diehl, G.E., Victorio, D.A., Huh, J.R., Galan, C., Miraldi, E.R., Swaminath, A., Bonneau, R., Scherl, E.J., and Littman, D.R. (2014). $CX_3CR1^+$ mononuclear phagocytes support colitis-associated innate lymphoid cell production of IL-22. J. Exp. Med. *211*, 1571–1583.

Martínez-Martínez, E., Gómez, I., Martín, P., Sánchez, A., Román, L., Tejerina, E., Bonilla, F., Merino, A.G., de Herreros, A.G., Provencio, M., and García, J.M. (2015). Cannabinoids receptor type 2, CB2, expression correlates with human colon cancer progression and predicts patient survival. Oncoscience *2*, 131–141.

Merad, M., Sathe, P., Helft, J., Miller, J., and Mortha, A. (2013). The dendritic cell lineage: ontogeny and function of dendritic cells and their subsets in the steady state and the inflamed setting. Annu. Rev. Immunol. *31*, 563.

Manta, C., Heupel, E., Radulovic, K., Rossini, V., Garbi, N., Riedel, C.U., and Niess, J.H. (2013). CX3CR1+ macrophages support IL-22 production by innate lymphoid cells during infection with Citrobacter rodentium. Mucosal Immunol. *6*, 177–188.

Newton, C.A., Chou, P.-J., Perkins, I., and Klein, T.W. (2009). CB(1) and CB(2) cannabinoid receptors mediate different aspects of delta-9-tetrahydrocannabinol (THC)-induced T helper cell shift following immune activation by Legionella pneumophila infection. J. Neuroimmune Pharmacol. *4*, 92–102.

Naftali, T., Bar-Lev Schleider, L., Dotan, I., Lansky, E.P., Sklerovsky Benjaminov, F., and Konikoff, F.M. (2013). Cannabis induces a clinical response in patients with Crohn's disease: a prospective placebo-controlled study. Clin. Gastroenterol. Hepatol. *11*, 1276–1280.e1.

Parks, O.B., Pociask, D.A., Hodzic, Z., Kolls, J.K., and Good, M. (2016). Interleukin-22 signaling in the regulation of intestinal health and disease. Front. Cell Dev. Biol. *3*, 85.

Polese, L., Angriman, I., Cecchetto, A., Norberto, L., Scarpa, M., Ruffolo, C., Barollo, M., Sommariva, A., and D'Amico, D.F. (2002). The role of CD40 in ulcerative colitis: histochemical analysis and clinical correlation. Eur. J. Gastroenterol. Hepatol. *14*, 237–241.

Pisanti, S., Picardi, P., D'Alessandro, A., Laezza, C., and Bifulco, M. (2013). The endocannabinoid signaling system in cancer. Trends Pharmacol. Sci. *34*, 273–282.

Persson, E.K., Uronen-Hansson, H., Semmrich, M., Rivollier, A., Hägerbrand, K., Marsal, J., Gudjonsson, S., Håkansson, U., Reizis, B., Kotarsky, K., and Agace, W.W. (2013). IRF4 transcription-factor-dependent CD103+CD11b+ dendritic cells drive mucosal T helper 17 cell differentiation. Immunity *38*, 958–969.

Roth, M.D., Castaneda, J.T., and Kiertscher, S.M. (2015). Exposure to δ9-tetrahydrocannabinol impairs the differentiation of human monocyte-derived dendritic cells and their capacity for T cell activation. J. Neuroimmune Pharmacol. *10*, 333–343.

Ramalingam, R., Larmonier, C.B., Thurston, R.D., Midura-Kiela, M.T., Zheng, S.G., Ghishan, F.K., and Kiela, P.R. (2012). Dendritic cell-specific disruption of TGF-β receptor II leads to altered regulatory T cell phenotype and spontaneous multiorgan autoimmunity. J. Immunol. *189*, 3878–3893.

Sun, D., Lin, Y., Hong, J., Chen, H., Nagarsheth, N., Peng, D., Wei, S., Huang, E., Fang, J., Kryczek, I., and Zou, W. (2015). Th22 cells control colon tumorigenesis through STAT3 and Polycomb Repression complex 2 signaling. Oncoimmunology *5*, e1082704.

Setiady, Y.Y., Coccia, J.A., and Park, P.U. (2010). In vivo depletion of CD4+FOXP3+ Treg cells by the PC61 anti-CD25 monoclonal antibody is mediated by FcgammaRIII+ phagocytes. Eur. J. Immunol. *40*, 780–786.

Singh, U.P., Singh, N.P., Singh, B., Price, R.L., Nagarkatti, M., and Nagarkatti, P.S. (2012). Cannabinoid receptor-2 (CB2) agonist ameliorates colitis in IL-10−/− mice by attenuating the activation of T cells and promoting their apoptosis. Toxicol. Appl. Pharmacol. *258*, 256–267.

Storr, M.A., Keenan, C.M., Zhang, H., Patel, K.D., Makriyannis, A., and Sharkey, K.A. (2009). Activation of the cannabinoid 2 receptor (CB2) protects against experimental colitis. Inflamm. Bowel Dis. *15*, 1678–1685.

Schulz, O., Jaensson, E., Persson, E.K., Liu, X., Worbs, T., Agace, W.W., and Pabst, O. (2009). Intestinal CD103+, but not CX3CR1+, antigen sampling cells migrate in lymph and serve classical dendritic cell functions. J. Exp. Med. *206*, 3101–3114.

Sun, C.-M., Hall, J.A., Blank, R.B., Bouladoux, N., Oukka, M., Mora, J.R., and Belkaid, Y. (2007). Small intestine lamina propria dendritic cells promote de novo generation of Foxp3 T reg cells via retinoic acid. J. Exp. Med. *204*, 1775–1785.

Uhlig, H.H., McKenzie, B.S., Hue, S., Thompson, C., Joyce-Shaikh, B., Stepankova, R., Robinson, N., Buonocore, S., Tlaskalova-Hogenova, H., Cua, D.J., and Powrie, F. (2006). Differential activity of IL-12 and IL-23 in mucosal and systemic innate immune pathology. Immunity *25*, 309–318.

Whiting, P.F., Wolff, R.F., Deshpande, S., Di Nisio, M., Duffy, S., Hernandez, A.V., Keurentjes, J.C., Lang, S., Misso, K., Ryder, S., et al. (2015). Cannabinoids for medical use: a systematic review and meta-analysis. JAMA *313*, 2456–2473.

**iScience, Volume *23***

## Supplemental Information

# Activation of Cannabinoid Receptor 2 Prevents Colitis-Associated Colon Cancer through Myeloid Cell De-activation Upstream of IL-22 Production

**William Becker, Haider Rasheed Alrafas, Kiesha Wilson, Kathryn Miranda, Courtney Culpepper, Ioulia Chatzistamou, Guoshuai Cai, Mitzi Nagarkatti, and Prakash S. Nagarkatti**

**Supplemental Figure 1: Representative flow cytometry gating strategies and colitis data related to Figure 2**

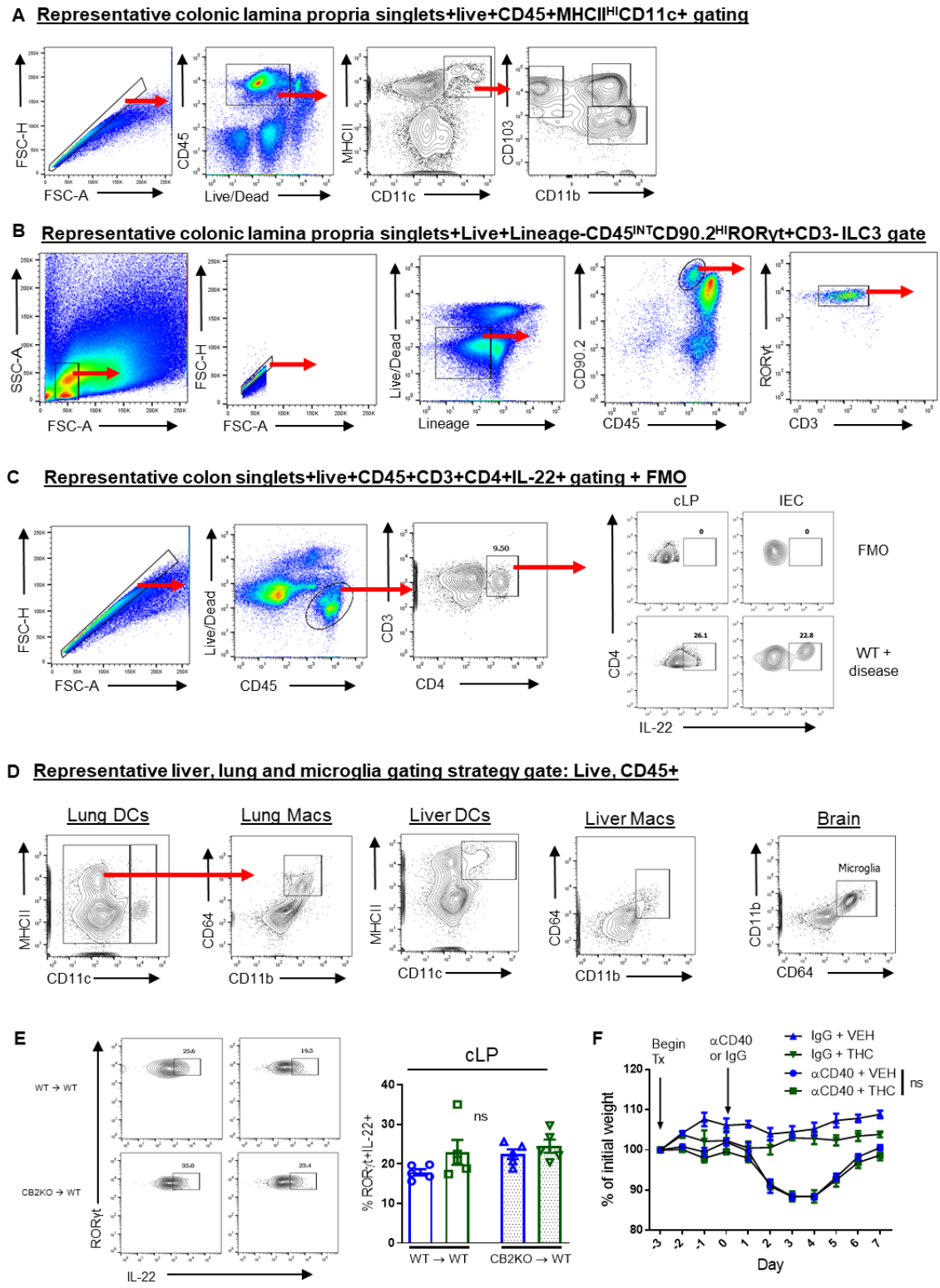

**(A-D)** Gating strategies for indicated cell types.

WT mice were myeloablated via two doses of 600 cGy separated by 3 hours then immune reconstitution was accomplished by transfer of bone marrow cells from WT (WT → WT) or Cnr2-/- CB2 knockout (CB2 → WT) mice.

**(E)** Flow cytometric analysis of RORγt+IL-22+ ILC3 (gate:Lineage-CD45$^{INT}$CD90.2$^{HI}$CD3-RORγt+) in the colonic lamina propria (n=4-5).

Each symbol represents an individual mouse. Data are from one experiment representative of two independent experiments and presented as mean ± SEM NS, not significant: ****p<0.0001 by Two-way ANOVA with Tukey's multiple comparisons test.

Mice were pre-treated daily with VEH or THC (10 mg/kg) for 3 days before intraperitoneal injection of rat anti-mouse IgG (control) or rat anti-mouse αCD40 (200 μg, clone FGK4.5 in PBS) and treatment continued for 7 days post disease induction to monitor progression of inflammatory severity.

**(F)** Percent weight change over the course of disease (n=3-10).

**Supplemental Figure 2: THC treatment reduces dendritic cell activation lessening the severity of αCD40 colitis, related to Figure 3.**

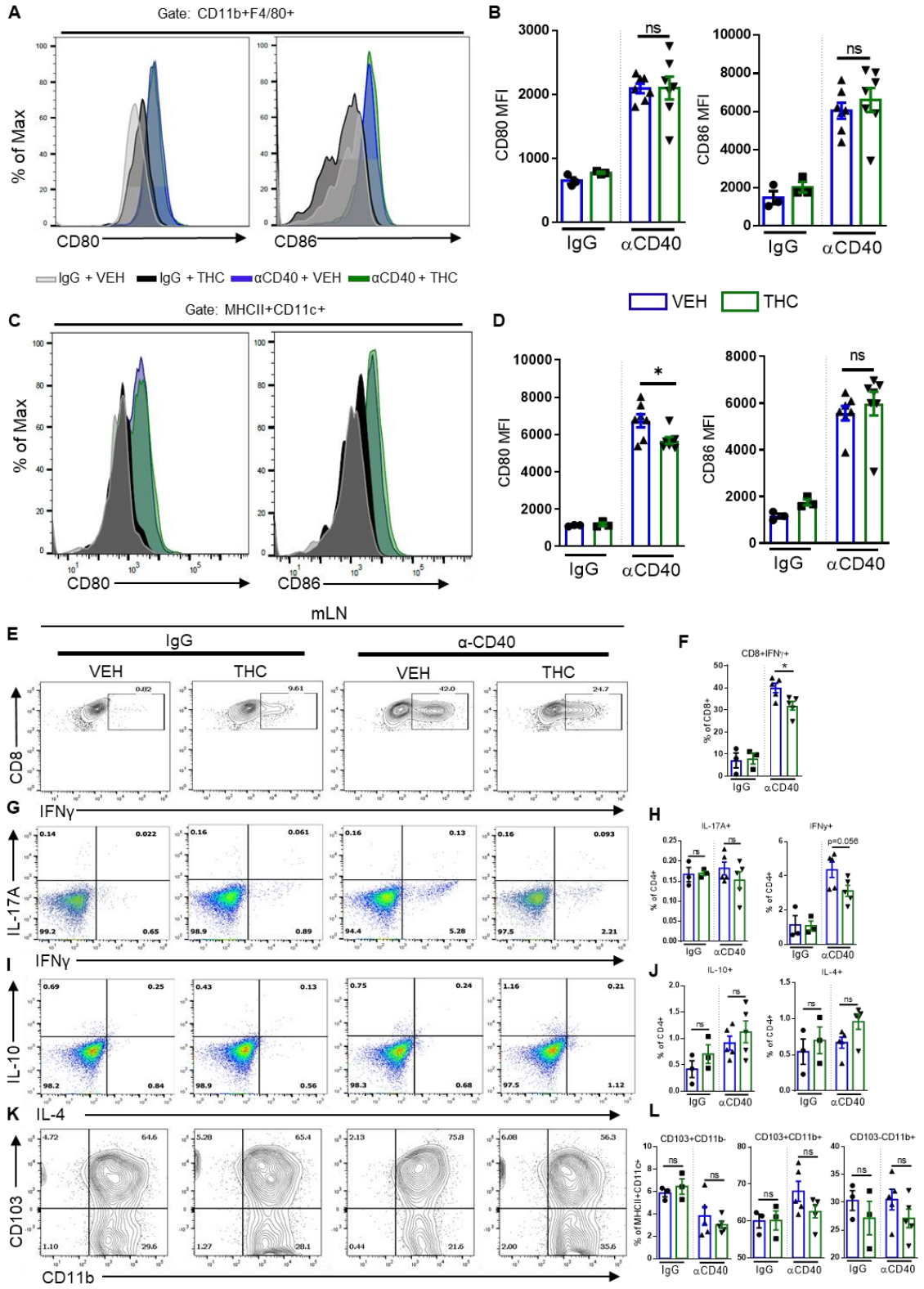

Mice were pre-treated for 3 days with VEH or THC before disease induction via i.p. injection of 200 μg anti-mouse αCD40 or IgG control. Treatments continued daily. At sacrifice, mLNs or cLPs were taken and analyzed by flow cytometry for immune cells of interest.

**(A**) Representative overlaid histograms displaying CD80 and CD86 expression in cLP macrophages, (gate: Live, CD45+CD11b+F4/80+), and in **(C)** cLP dendritic cells (gate: Live, CD45+MHCII$^{HI}$CD11c+).

**(E, G, I, K)** Representative flow cytometry plots from the mLN of **(E)** CD8+IFNγ+ cells (gate: CD3+CD4-CD8+); **(G)** IL-17A and IFNγ single and double positive cells (gate: CD3+CD4+); **(I)** IL-10 and IL-4 positive cells (gate: CD3+CD4+); and **(K)** dendritic cell subsets (gate: MHCII$^{HI}$CD11c+).

**(B, D, F, H, J, L)** Quantification of flow cytometry results (n=3 IgG groups, n=5-7 αCD40 groups).

Data are presented as mean ± SEM of two independent experiments. NS, not significant: *P<0.05, **P<0.01, ****P<0.0001 by Two-way ANOVA with Tukey's multiple comparisons test.

**Supplemental Figure 3: THC reduces pro-inflammatory DCs, and t-SNEs related to Figure 5**

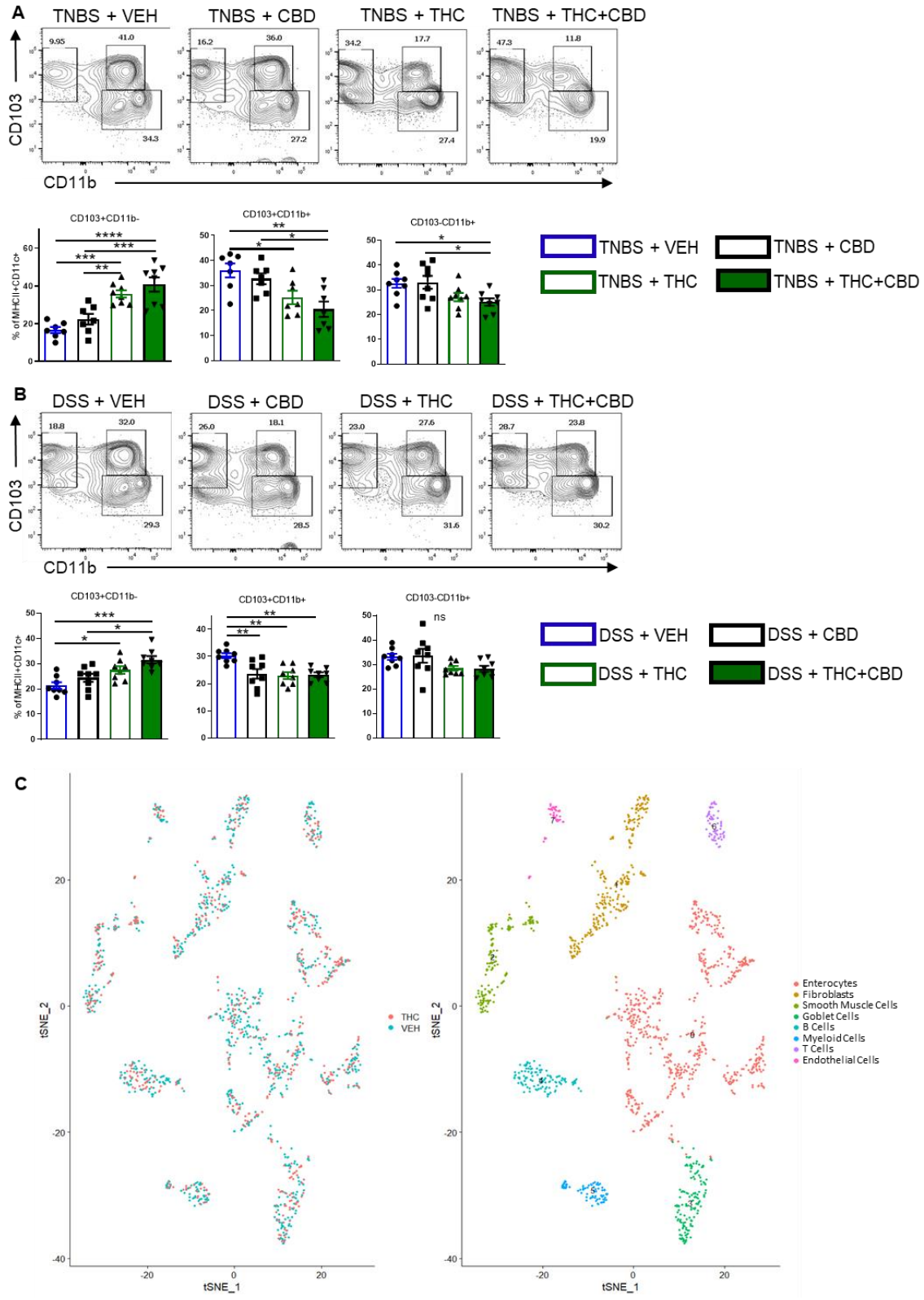

BALB/c mice were injected intrarectally with 100 mg/kg TNBS in 50% ethanol. Starting three days before disease induction and continuing daily, mice were gavaged with either: Vehicle (10% EtOH in PBS+Tween-80), CBD (10 mg/kg), THC (10mg/kg) or a combination of THC and CBD (10 mg/kg, both). **(A**) Representative flow cytometry contour plots of cLP dendritic cell subsets at sacrifice (gate: Live,CD45+,MHCII$^{HI}$CD11c+) (n=7).

C57BL/6 mice were treated with either: Vehicle, CBD (10 mg/kg), THC (10mg/kg) or a combination of THC and CBD (10 mg/kg, both) for 3 days before 2% DSS was added to their drinking water. DSS remained in the drinking water until termination of the study 14 days later. Mice were sacrificed at 14 days post disease induction and cLP was isolated and stained for markers of dendritic cell phenotype CD103 and CD11b.

**(B)** Representative contour plots of cLP dendritic cell subsets at sacrifice (gate: Live,CD45+,MHCII$^{HI}$CD11c+) (n=7-8).

WT mice were administered VEH or THC (10mg/kg) by oral gavage and 24 hours later colons were isolated.

**(C)** scRNA-seq tSNE plots of colon cell clustering from an aggregated sample of colon lamina propria-enriched cells 24 hours after VEH or THC administration.

Data are presented as mean ± SEM. NS, not significant: *P<0.05, **P<0.01, ****P<0.0001 Two-way ANOVA with Tukey's multiple comparisons test (**A,B, D**).

**Supplemental Figure 4: THC reduces pro-inflammatory DCs and decreases CD86 expression to reduce T cell responses, related to Figures 5 and 6.**

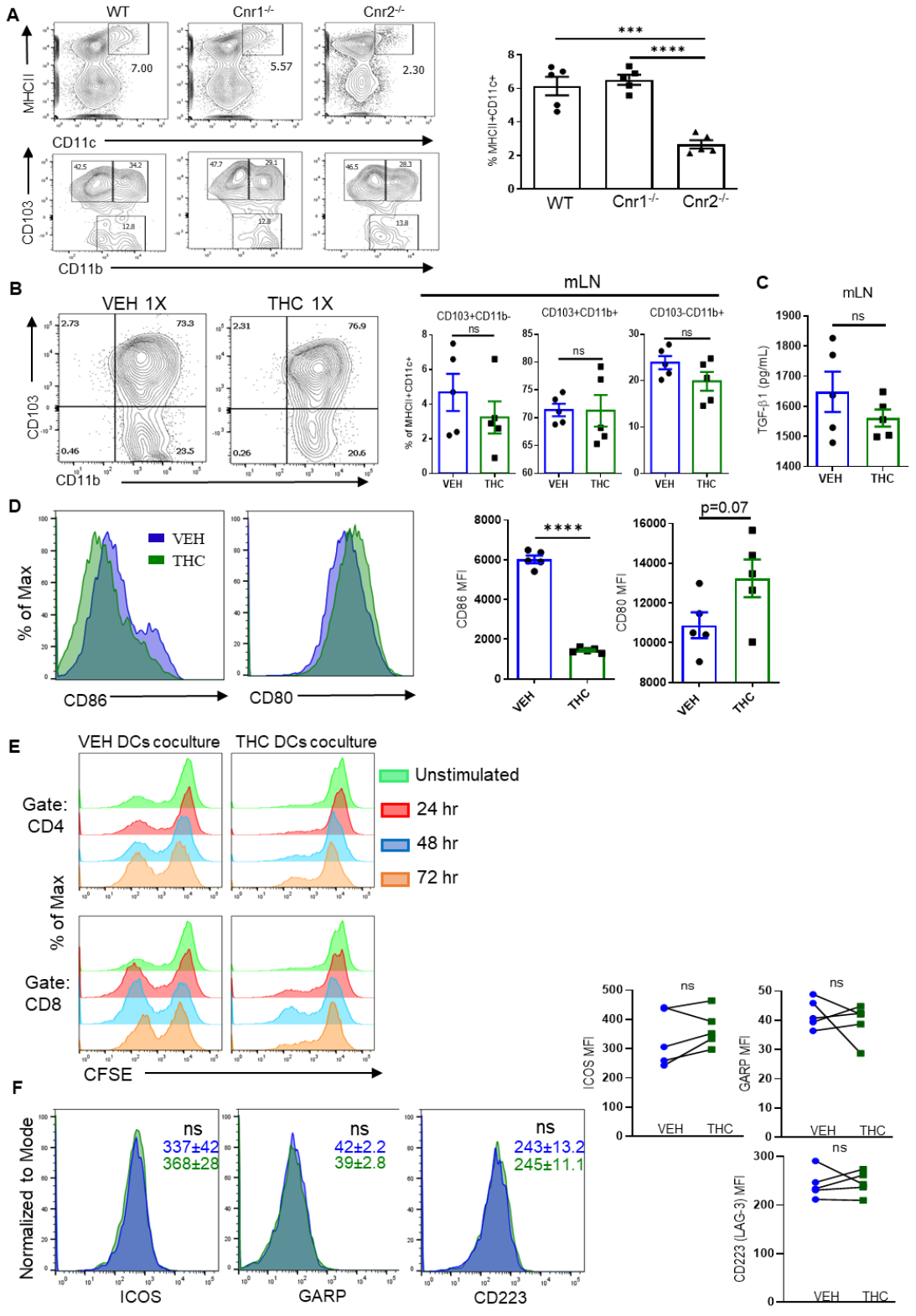

**(A)** Naïve WT, $Cnr1^{-/-}$, and $Cnr2^{-/-}$ mice were given one administration of VEH or THC and 24 hours later cLP was harvested and analyzed via flow cytometry for DCs and their expression of CD103 and CD11b.

Naïve WT mice were given VEH or THC (10mg/kg) and mLNs were collected 24 hours later.

**(B)** Representative flow cytometry contour plot of mLN DC phenotype (gate: LiveCD45+MHCII+CD11c+).

**(C)** 1x10^6 cells from the mLNs of VEH or THC treated mice were plated overnight and supernatants were subjected to ELISA for TGF-β1.

**(D)** Representative overlaid histograms of CD80 and CD86 expression gated on dendritic cells ($MHCII^{HI}CD11c+$).

After 6 days of BMDC generation, CD11c+ cells were selected from wells treated with either THC or VEH and then co-cultured with naïve CFSE-pulsed CD3+ T cells at a ratio of 1:5, DCs : T cells. Un-stimulated wells received 50µg of IgG control antibody, while experimental groups received 50µg of anti-CD40. Cells were collected daily for flow cytometric analysis of CFSE dilution among CD4 and CD8 T cell subsets after being co-cultured with VEH or THC treated DCs.

**(E)** Representative offset histograms of CFSE expression gated on CD4 cells (upper panel) or CD8 (lower panel) after incubation with VEH or THC treated DCs and stimulated with IgG (control – unstimulated), or anti-CD40.

**(F)** Representative overlaid histograms and median fluorescence intensity of ICOS, GARP and CD223 (LAG-3) expression on Tregs cultured with VEH or THC.

Data are presented as mean ± SEM. NS, not significant: *P<0.05, **P<0.01, ****P<0.0001 by Students *t*-test.

**Supplemental Figure 5: THC administration causes cLP immune cell phenotype changes through CB2, related to Figure 6.**

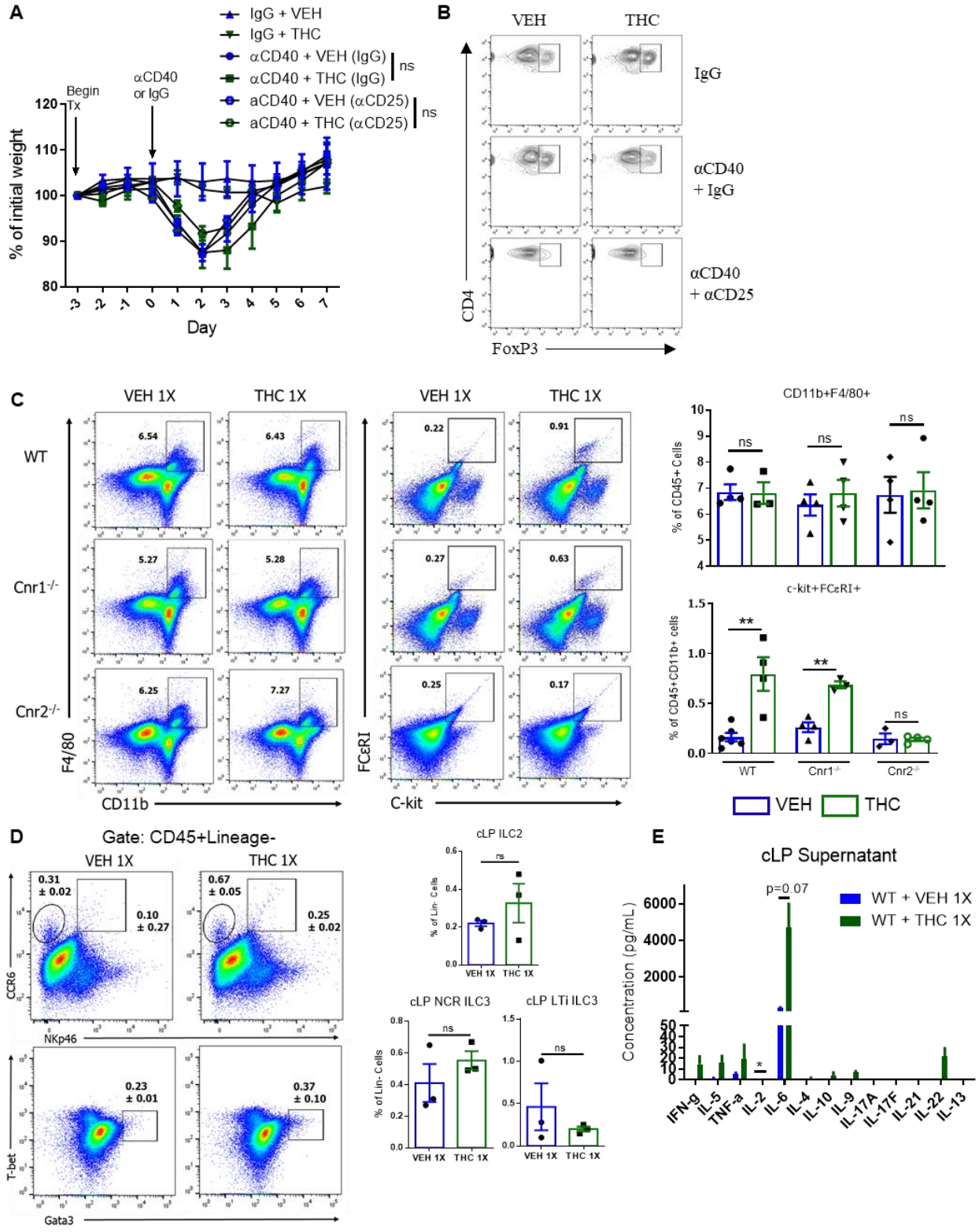

10 days before disease induction Treg were depleted via i.p. injection of rat anti-mouse CD25 (clone PC61, 250 μg/mouse) or isotype control. Mice were pre-treated with VEH or THC (10mg/kg) for 2 days before disease induction by i.p. injection of αCD40 or IgG control.

**(A**) Body weight throughout disease course.

**(B)** Representative flow cytometry contour plots of CD4+FoxP3+ T regulatory cells (gate: CD45+CD4+) in the mLN of indicated mice at sacrifice.

Naïve WT, Cnr1$^{-/-}$, and Cnr2$^{-/-}$ mice were given one administration of VEH or THC and 24 hours later cLP was harvested and analyzed via flow cytometry for immune cell populations of interest.

**(C)** Representative pseudocolor dot plots displaying CD11b+F4/80+ macrophages (gate: Live, CD45+), and FCεRI+C-kit+ mast cells (gate: Live, CD45+CD11b+) in the cLP (n=4 per group).

**(D)** Flow cytometry dot plots showing NCR ILC3s (Lineage-CCR6+NKp46+), LTi ILC3s (Lineage-CCR6+NKp46-) and ILC2s (Lineage-Gata3+) (n=3).

**(E)** 1x10$^6$ live cLP cells from the indicated groups were plated overnight, supernatants were collected, and subjected to Legendplex assay for Mouse T helper cytokines (n=2 per group). Data are presented as mean ± SEM. *P<0.05, **P<0.01, ****P<0.0001 by Students *t*-test.

**Supplemental Figure 6: THC reduction of APC activation markers, related to Figure 7.**

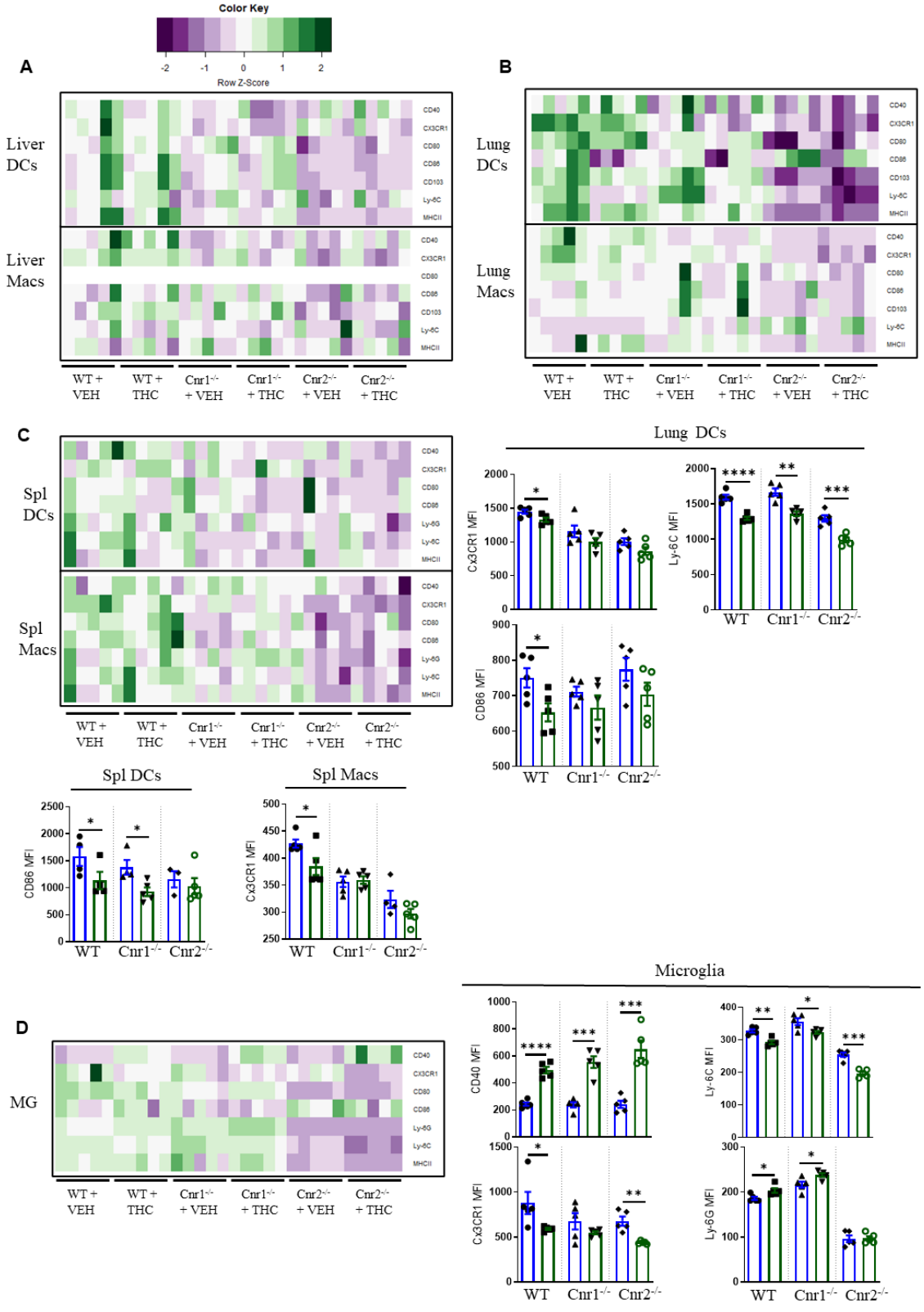

Naive age and sex-matched WT, $Cnr1^{-/-}$, and $Cnr2^{-/-}$ mice were euthanized and colonic lamina propria (cLP), mesenteric lymph nodes (mLNs), spleens (spl), livers, lungs and brain were brought to a single cell suspension and then treated *ex-vivo* with either VEH or THC (10μM) for 18 hours before being analyzed for markers of antigen-presenting cell (APC) activation by flow cytometry.

**(A-D)** Heatmap of median fluorescence intensities of (in descending order) CD40, CX3CR1, CD80, CD86, Ly-6G, Ly-6C, and MHCII on macrophages and dendritic cells from tissues deriving from WT, $Cnr1^{-/-}$, or $Cnr2^{-/-}$ mice treated with VEH or THC and quantification of flow cytometry results (n=5).

Each symbol represents a different mouse. Data are presented as mean ± SEM. *P<0.05, **P<0.01, ****P<0.0001 by Two-way ANOVA with Tukey's multiple comparisons test.

**Supplemental Figure 7: THC does not alter body weight loss in SCID mice given αCD40, related to Figure 8.**

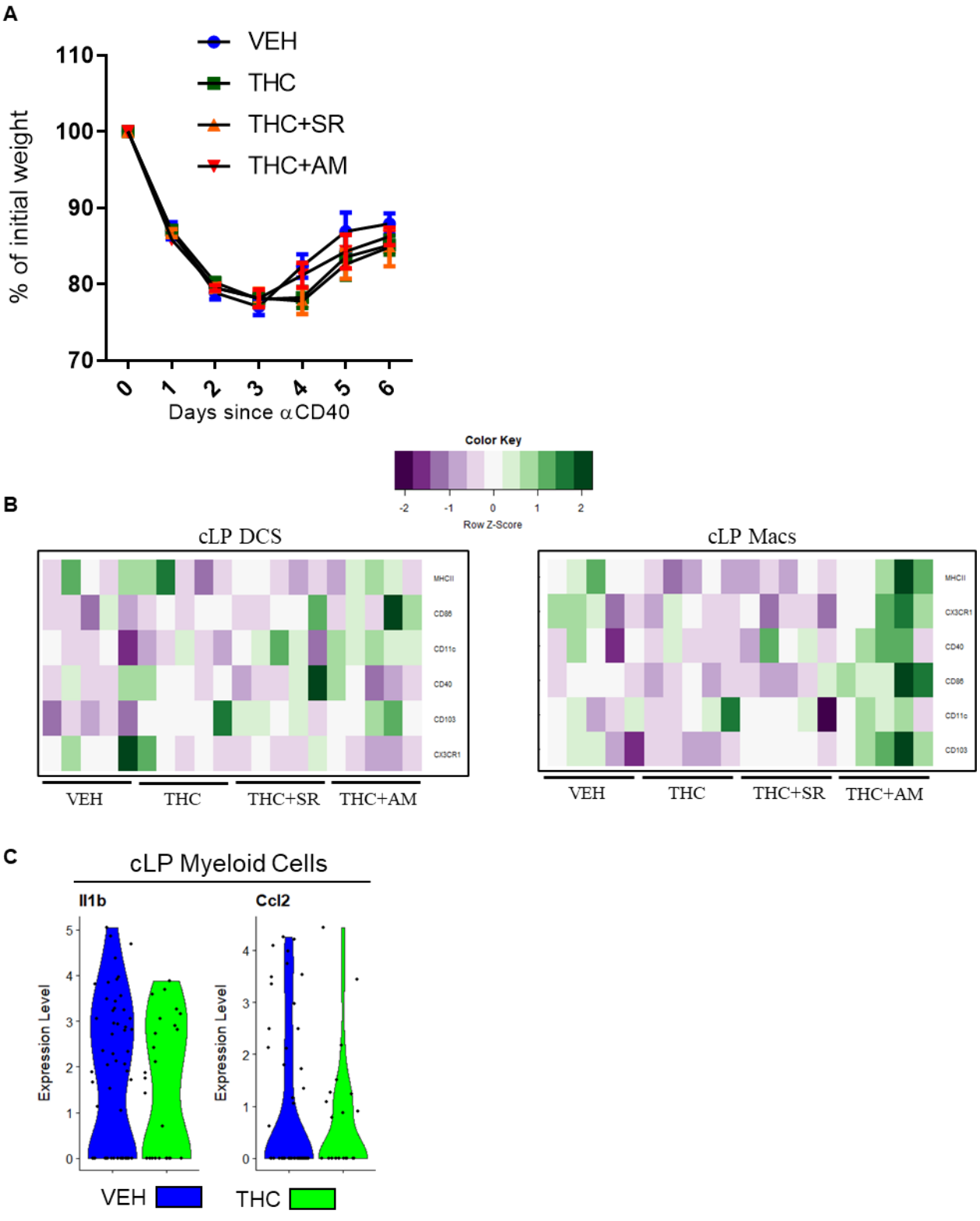

SCID mice were injected with rat anti-mouse αCD40 (200 μg, clone FGK4.5 in PBS) and received either VEH, THC (10mg/kg), THC+SR144528 (THC+SR, 10mg/kg, both) or THC+AM251 (THC+AM, 10mg/kg, both) daily for 7 days.

**(A**) Body weight throughout disease course.

**(B)** Heatmap of median fluorescence intensity of indicated markers in cLP DCs and cLP Macs.

**(C)** scRNA-seq violin plot of indicated mRNA expression in the myeloid cell cluster from the colon of mice treated with VEH or THC for 24 hours.

## Transparent Methods

*Mice.* The University of South Carolina Institutional Animal Care and Use Committee approved all experiments. All mice were housed at the AAALAC-accredited animal facility at the University of South Carolina, School of Medicine (Columbia, SC) under specific pathogen-free conditions and 12 hr dark/light cycles in temperature-controlled rooms and given *ad libitum* access to water and normal chow diet. Female C57BL/6 and B6.CB17-*Prkdc*$^{scid}$/SzJ mice aged 8-12 weeks were obtained from Jackson Laboratories (Bar Harbor, ME, USA). Cnr1$^{-/-}$ and Cnr2$^{-/-}$ mice are on a C57BL/6 background and were bred and maintained in-house. Female and male mice were used for *in vitro* experiments. The number of mice for each experimental cohort is described in the figure legends.

*anti-CD40 colitis induction and treatments.* To induce anti-CD40 colitis, mice were injected i.p. with 100 μL of 200 μg of anti-CD40 IgG2a monoclonal antibody (clone FGK4.5) or isotype rat IgG2a control (both from Bio X Cell), dissolved in PBS. Treatment with vehicle control (2:1:18 ethanol:Tween-80:PBS) or THC (10mg/kg) began 3 days before disease induction unless otherwise indicated. Studies examining the effects of Treg depletion on anti-CD40 colitis progression proceeded as above but with an i.p. injection of rat anti-mouse CD25 (clone PC61, 250 μg/mouse) or isotype control (both from Biolegend) one week before anti-CD40 injection. Tregs were confirmed to be depleted via flow cytometric analysis of reduced FoxP3+ Tregs in the blood, mLNs and spleens.

*AOM/DSS model of colitis and colitis-induced colorectal cancer*. C57BL/6 mice aged 8-10 weeks old were injected i.p. with azoxymethane (AOM, MPBIO) (10mg/kg). DSS (1%) was added to the drinking water one week after AOM administration for one week before regular drinking water was returned for two weeks. Three DSS (1%)-regular water cycles were completed before mice were kept on regular water and monitored for polyps via colonoscopy. Treatments with VEH or THC (10mg/kg) began one week after administration of AOM and continued twice weekly until the end of the last DSS cycle. For studies investigating the contribution of CB2 on hematopoietic cells to THC-mediated AOM-DSS-induced colitis prevention, six to eight week old female C57BL/6 WT mice were myeloablated via two doses of 600 cGy

separated by 3 hours then immune reconstitution was accomplished by transfer of bone marrow cells from WT (WT → WT) or Cnr2-/-, CB2 knockout (CB2 → WT) mice. One month after bone marrow reconstitution, the AOM–DSS murine model for colorectal tumorigenesis was induced by a single i.p. injection of AOM (10mg/kg), on day 3 treatment with THC (10mg/kg) or VEH began that continued until study termination, and on day 5, a 5-day DSS cycle (2%) was administered in the water.

*TNBS and DSS colitis induction and treatments.* For all colitis experiments, unless otherwise indicated, treatments began three days before disease induction with CBD (10mg/kg), THC (10mg/kg) or a combination of THC+CBD (10mg/kg, both), or the vehicle control. All treatments were suspended in ethanol and delivered to animals as a ratio of 2:1:18 ethanol:Tween-80:PBS by oral gavage. For the induction of TNBS-induced colitis, BALB/C mice were anesthetized by light isofluorane administration and given an intrarectal administration of 100 μL of 1mg of TNBS (Millipore, Sigma) dissolved in 50% ethanol. Mice were kept vertical for 30s after TNBS administration to keep the TNBS in contact with the colonic mucosal surface. DSS colitis was induced by dissolving 2% DSS (MP Biomedicals) in the drinking water and giving mice *ad libitum* access until the end of the study or humane endpoints were reached.

*Assessment of colitis disease parameters.* For all colitis models, mice were weighed daily, and colon lengths were measured at experimental end-points. Colonoscopy images were taken at indicated time points by anesthetizing the mice and using a high-resolution mouse endoscopic system Karl Storz (Tuttlingen, Germany) Tele Pack Vet X LED endoscope designed for small animals. The severity of colitis was scored using the mouse endoscopy and murine endoscopic index of colitis severity (MEICS) system, detailed in **Table 1**.

*Histology and Tissue Scoring*. Proximal colon tissues were excised, rinsed with PBS and fixed by immersion in 3% paraformaldehyde (PFA) for 24 hours. Fixed tissues were embedded in paraffin, sectioned and stained with hematoxylin and eosin. Color bright field images and picture montages were taken using a Cytation-5 Imaging Reader (BioTek Instruments, Winooski, VT, USA).

Colon tissues were scored for severity of disease by a pathologist according to four criteria (Bouchlaka et al., 2013): Epithelial hyperplasia, goblet cell depletion, lamina propria infiltrate and epithelial cell damage. For all parameters; 0 = no pathology, 1 = mild, 2 = intermediate, 3 = severe changes. Liver tissues were scored according to the degree of necroinflammation (Bouchlaka et al., 2013, Thoolen et al., 2010, Goodman, 2007): 0 = no necrosis, 1 = minimal centrilobular necrosis, 2 = extensive centrilobular necrosis, 3 = bridging necrosis (necrosis extending to portal tracts), 4 = patchy irregular necrosis (irregular patchy areas of coagulative necrosis with infiltration of inflammatory cells. There is not a lobular pattern of necrosis).

*Tissue Processing.* Mesenteric lymph nodes (MLNs) and spleens were excised and brought to a single cell suspension. Spleens were subjected to red blood cell lysis before both spleens and MLNs were passed through a 70 μM filter, spun down and re-suspended in FACS buffer for flow-cytometric analyses.

To isolate the colonic lamina propria (cLP), colons were excised and luminal contents were removed by gliding curved forceps down the length of the colon, colons were opened longitudinally and mucus was removed by gentle scraping in sterile 1X PBS. Tissue was cut into 0.5 cm pieces and incubated in pre-warmed sterile 1X HBSS (without Ca2+ and Mg2+) containing FBS (3%vol/vol), 10mM EDTA (Cellgro), and 5mM DL-Dithiotreitol (DTT; MilliporeSigma) for 30 minutes at 37°C while shaking. The intra-epithelial cells (IECs) containing immune cells and enterocytes were recovered by filtering the colon pieces over a 100μM filter. The supernatant containing the IEC fraction was put on ice for at least 10 minutes to allow sedimentation of debris, and the IEC fraction was taken from the upper part of the supernatant. Remaining tissue containing the cLP was incubated in pre-warmed 1X HBSS (with Ca2+ and Mg2+) solution (15mL/colon) containing FBS (3%vol/vol), 1% L-glutamine, 1% penicillin–streptomycin, 10 mM HEPES, 0.5 mg/mL collagenase D (Roche), 0.5 mg/mL Dispase (MilliporeSigma) and 0.04 mg/mL DNase I (MilliporeSigma) for 45 minutes at 37°C while shaking. The supernatant was filtered over a 70μm cell strainer into ice cold sterile 1X PBS. cLP cells were passed through a Percoll (GE Healthcare) gradient (40%/80%(v/v) gradient) and spun at 620xg for 20 minutes

with low acceleration and no brake. Cells at the 40/80 interface were collected and washed twice with supplemented FACS buffer and prepared for flow cytometric analysis.

To isolate liver and lung mononuclear cells, mice were perfused with 10mL of heparinized PBS, then whole tissues were extracted, subjected to enzymatic digestion in FACS buffer with 2mg/mL (w/v) Collagenase type IV (MilliporeSigma) for 30 minutes at 37°C with light shaking before physical dissociation in FACS buffer. Samples were spun down and passed over 100μM filters then passed through a 40%/80% Percoll gradient and cells at the interface were collected and washed as was done with cLP cells.

Whole brain was homogenized via Neural Tissue Dissociation Kit (Miltenyi Biotech). Mononuclear cells from were then isolated by centrifugation in media containing 33% (v/v) isotonic Percoll in FACS buffer (1X PBS, 2% heat-inactivated fetal bovine serum) (GE Healthcare). Pelleted cells were washed twice with FACS buffer before being plated overnight in complete media.

*Single Cell RNA-seq and Analysis.* Cell number and viability from cLP samples were measured using a TC20 Automated Cell Counter (BioRad). Processed samples showed at least 80% viability. Cells were then loaded onto the Chromium Controller (10x Genomics) targeting 1000 cells per lane. The Chromium v2 single cell 3′ RNA-seq reagent kit (10x Genomics) was used to process samples into single cell RNA-seq libraries according to the manufacturer's protocol. Libraries were sequenced with a NextSeq 550 instrument (Illumina) with a depth of 40k–60k reads per cell. The 10x Genomics Cell Ranger pipeline (version 2.0) was used to generate FASTQ files, align reads to mm10 genome and summarize read count for each gene in each single cell. Downstream analysis was completed using R scripts and Seurat suite version 3.0 (https://satijalab.org/seurat/). Data was integrated in Seurat using anchor and integration function. The integrated data was scaled and Principal-component analysis (PCA) was completed for dimensionality reduction. Clusters were made following PCA analysis by adjusting the granularity resolution to 0.15. We determined the number of principal components (PCs) to utilize post JackStraw analysis within Seurat to determine PCs with the lowest P-value. Differential expression was determined

for each cluster to determine cluster biomarkers, and between the VEH and THC samples using the default Wilcoxon rank sum test. Raw sequencing data is available at the Sequence Read Archive (SRA), accession: PRJNA592156, and processed data files are available at Gene Expression Omnibus (GEO) accession number: GSE155669.

*Flow cytometry.* Relevant tissues were brought to a single cell suspension, then 1-2 x $10^6$ cells were washed with PBS and then stained with Live/Dead Fixable Aqua Dead Cell Stain Kit (Invitrogen) for 30 minutes at 4°C. Cells were then washed and incubated with TruStain FcX anti-mouse CD16/32 (Biolegend) to block Fc receptors. Extracellular antigens were stained for 20 minutes at room temperature in staining buffer. Cells were fixed and permeabilized with BD Cytofix/Cytoperm (for cytokine restimulations) or BD Transcription Factor Buffer Set (for transcription factor staining) per manufacturer's instructions. Intracellular antigens were stained for 1 hour at 4°C in the appropriate 1x Perm/Wash buffer. Cells were washed with staining buffer and passed through a 100 μm nylon mesh before acquisition on a BD FACSCelesta (Becton Dickinson). Analysis was performed using FlowJo software (FlowJo, BD). All samples were recorded based on the same live cell threshold per tissue. Compensation was set using UltraComp eBeads (Invitrogen). Fluorochrome-conjugated antibodies are detailed in **Table 2**.

*Cell culture and in vitro treatments.* Cells were cultured in a sterile incubator maintained at 37°C and 5% CO2. Primary cells were cultured in complete RPMI supplemented with 10% FBS, 100 U/mL penicillin, 100 U/mL streptomycin, 10mM HEPES (Gibco, Paisley, UK), and 50 μM β-mercaptoethanol (MilliporeSigma, Gillingham, UK) (complete medium). Th22 polarization was performed by magnetic bead separation of naïve CD4+ T cells from spleens and lymph nodes of 8 week old female C57BL/6 mice then plating cells in the presence of anti-mouse CD3ε (1μg/mL), anti-mouse CD28 (4μg/mL), Il-1β (10ng/mL), Il-6 (30ng/mL), IL-23 (20ng/mL) (all from Biolegend), FICZ (400nM, Sigma) and anti-TGF-β (5μg/mL, R&D Systems) for 3 days. For Th0 polarization, cells were stimulated with anti-mouse CD3ε and anti-mouse CD28.

*Bone marrow dendritic cell generation and DC: T cell coculture.* Naïve bone marrow cells were collected from the femurs of 10-week-old C57BL/6 mice and plated at a density of $1x10^6$ cells/mL in 24-well plates with GM-CSF (20ng/mL) and IL-4 (10 ng/mL) supplementation to generate bone-marrow dendritic cells (BMDCs). 18 hours after initial plating, debris and non-adherent cells were removed and media containing GM-CSF was replaced and cells were monitored for 7 days until the end of culture. VEH or THC (10μM) were added to wells at initial plating and at media changes. On day 7, floating cells were collected and analyzed by flow cytometry, recovered supernatants were subjected to ELISA for TGF-β1. On day 6, floating cells were collected and DCs were purified by magnetic sorting for CD11c (EasySep, STEMCELL Technologies). Some purified DCs were re-plated in complete media for another day before supernatants were collected. Concurrently, naïve C57BL/6 mice were sacrificed, spleens and lymph nodes were harvested and brought to a single cell suspension before CD3+ T cells were isolated via magnetic sorting and pulsed with CFSE (5μM). CD11c purified BMDCs treated with VEH or THC were plated with naïve T cells in 48-well plates at a ratio of 1:5 DCs to T cells with either 50 μg IgG control (Biolegend) or 50 μg anti-CD40 (BioXCell). Co-cultures continued for 3 days and select wells were harvested daily for examination of T cell proliferation.

*Statistical Analyses* Data were analyzed using GraphPad Prism software with the statistical test and number of experimental repetitions indicated in the respective figure legends. Unless otherwise stated, data are presented as individual dots for each sample/mouse, a line for mean, and bars indicating SEM. Tests were always 2-sided where applicable; $P < 0.05$ was considered significant. Heatmaps were generated using the ggplot2 package in R (version 3.6.2).

*Materials Availability Statement* This study did not generate new unique reagents.

**Table 1. Mouse endoscopy and murine endoscopic index of colitis severity (MEICS).**

| Parameter | Description | Score |
|---|---|---|
| Translucency of the Colon Mucosa | Transparent | 0 |
| | Moderate | 1 |
| | Marked | 2 |
| | Non-transparent | 3 |
| Vascular Patter | Normal | 0 |
| | Moderate | 1 |
| | Marked | 2 |
| | Bleeding | 3 |
| Fibrin Visible | None | 0 |
| | Little | 1 |
| | Marked | 2 |
| | Extreme | 3 |
| Stool Consistency | Normal + solid | 0 |
| | Still shaped | 1 |
| | Unshaped | 2 |
| | Spread | 3 |

**Table 2. List of Reagents**

| Antibody | Clone | Identifier | Source |
|---|---|---|---|
| APC/Cy7 anti-mouse CD45 Antibody | 30-F11 | 103115 | Biolegend |
| Brilliant Violet 785™ anti-mouse CD4 Antibody | GK1.5 | 100453 | Biolegend |
| Brilliant Violet 421™ anti-mouse FOXP3 Antibody | MF-14 | 126419 | Biolegend |
| Mouse Neuropilin-1 Alexa Fluor® 488-conjugated Antibody | 761704 | FAB59941G | R&D Systems |
| Alexa Fluor® 700 anti-mouse/human CD11b Antibody | M1/70 | 101222 | Biolegend |
| PE anti-mouse CD4 Antibody | GK1.5 | 100407 | Biolegend |
| APC/Fire™ 750 anti-mouse CD40 Antibody | 3/23 | 124631 | Biolegend |
| Brilliant Violet 650™ anti-human/mouse/rat CD278 (ICOS) Antibody | C398.4A | 313549 | Biolegend |
| Alexa Fluor® 647 anti-mouse GARP (LRRC32) Antibody | F011-5 | 142905 | Biolegend |
| BV650 Rat Anti-Mouse CD223 | C9B7W | 740560 | BD Biosciences |
| Alexa Fluor® 700 anti-mouse CX3CR1 Antibody | SA011F11 | 149035 | Biolegend |

| | | | |
|---|---|---|---|
| Alexa Fluor® 700 anti-mouse Lineage Cocktail | 17A2/ RB6-8C5/ RA3-6B2/ Ter-119/M1/70 | 133313 | Biolegend |
| Brilliant Violet 605™ anti-mouse CD11c Antibody | N418 | 117334 | Biolegend |
| PerCP/Cyanine5.5 anti-mouse CD103 Antibody | 2E7 | 121416 | Biolegend |
| Brilliant Violet 421™ anti-mouse F4/80 Antibody | BM8 | 123137 | Biolegend |
| PE/Dazzle™ 594 anti-mouse CD117 (c-Kit) Antibody | 2B8 | 105834 | Biolegend |
| PerCP anti-mouse CD8a Antibody | 53-6.7 | 100732 | Biolegend |
| PE anti-mouse FcεRIα Antibody | MAR-1 | 134308 | Biolegend |
| PE anti-mouse Ly-6G/Ly-6C (Gr-1) Antibody | RB6-8C5 | 108407 | Biolegend |
| Alexa Fluor® 647 anti-mouse I-A/I-E Antibody | M5/114.15.2 | 107617 | Biolegend |
| PE Mouse anti-Mouse RORγt | Q31-378 | 562607 | BD Biosciences |
| Brilliant Violet 605™ anti-T-bet Antibody | 4B10 | 644817 | Biolegend |
| PE/Dazzle™ 594 anti-mouse/human Helios Antibody | 22F6 | 137232 | Biolegend |

| | | | |
|---|---|---|---|
| PE/Dazzle™ 594 anti-mouse CD196 (CCR6) Antibody | 29-2L17 | 129822 | Biolegend |
| Brilliant Violet 510™ anti-mouse CD335 (NKp46) Antibody | 29A1.4 | 137623 | Biolegend |
| FITC anti-mouse IL-17A Antibody | TC11-18H10.1 | 506907 | Biolegend |
| Brilliant Violet 605™ anti-mouse IL-10 Antibody | JES5-16E3 | 505031 | Biolegend |
| Brilliant Violet 421™ anti-mouse IL-4 Antibody | 11B11 | 504127 | Biolegend |
| Brilliant Violet 650™ anti-mouse IFN-γ Antibody | XMG1.2 | 505832 | Biolegend |
| PE/Dazzle™ 594 anti-mouse CD197 (CCR7) Antibody | 4B12 | 120122 | Biolegend |
| BV786 Rat Anti-Mouse CD103 | M290 | 564322 | BD Biosciences |
| BB700 Rat Anti-Mouse I-A/I-E | M5/114.15.2 | 746197 | BD Biosciences |
| TruStain FcX™ (anti-mouse CD16/32) Antibody | 93 | 101320 | Biolegend |

| **Antibody or Reagent** | **Dose & Route of Administration** | **Catalog Number** | **Source** |
|---|---|---|---|
| Dextran Sulfate Sodium Salt (DSS) - Colitis Grade (36,000-50,000 MW) | Drinking water (2% wt/vol) | 0216011080 | MPBIO |

| | | | |
|---|---|---|---|
| Picrylsulfonic acid solution (TNBS) | | P2297 | Millipore-Sigma |
| InVivoMAb anti-mouse CD40 (Clone FGK4.5) | 200 μg, i.p. | BE0016-2 | BioXCell |
| InVivoMAb rat IgG2a isotype control, anti-trinitrophenol (Clone 2A3) | 200 μg, i.p. | BE0089 | BioXCell |
| Ultra-LEAF™ Purified anti-mouse CD25 Antibody (Clone PC61) | 250 μg/mouse, i.p. | 102040 | Biolegend |
| Ultra-LEAF™ Purified Rat IgG1, κ Isotype Ctrl Antibody (Clone RTK2071) | 250 mg/kg, i.p. | 400432 | Biolegend |
| Δ9-Tetrahydrocannabinol solution | 10 mg/kg, oral gavage | T2386 | Millipore Sigma |
| Δ9-THC | 10 mg/kg, oral gavage | *12068* | Cayman Chemical |
| Cannabidiol | 10 mg/kg, oral gavage | 90080 | Cayman Chemical |
| SR 144528 | 10 mg/kg, oral gavage | 5039 | Tocris |
| AM 251 | 10 mg/kg, oral gavage | 1117 | Tocris |

| | | | |
|---|---|---|---|
| Recombinant Mouse GM-CSF (carrier-free) | 20 ng/mL | 576304 | Biolegend |
| Recombinant Mouse IL-4 (carrier-free) | 10 ng/mL | 574304 | Biolegend |
| CFSE Cell Proliferation Kit | 5 μM | C34554 | Invitrogen |

**References:**

Bouchlaka, M. N. *et al.* Aging predisposes to acute inflammatory induced pathology after tumor immunotherapy. *J Exp Med* **210**, 2223–2237 (2013).

Thoolen, B. *et al.* Proliferative and nonproliferative lesions of the rat and mouse hepatobiliary system. *Toxicol Pathol* **38**, 5S-81S (2010).

Goodman, Z. D. Grading and staging systems for inflammation and fibrosis in chronic liver diseases. *Journal of Hepatology* **47**, 598–607 (2007).